

Matrix Formulae for Decorated Super Teichmüller Spaces

Gregg Musiker, Nicholas Ovenhouse, and Sylvester W. Zhang

ABSTRACT. For an arc on a bordered surface with marked points, we associate a holonomy matrix using a product of elements of the supergroup $\mathrm{OSp}(1|2)$, which defines a flat $\mathrm{OSp}(1|2)$ -connection on the surface. We show that our matrix formulas of an arc yields its super λ -length in Penner-Zeitlin's decorated super Teichmüller space. This generalizes the matrix formulas of Fock-Goncharov and Musiker-Williams. We also prove that our matrix formulas agree with the combinatorial formulas given in the authors' previous works. As an application, we use our matrix formula in the case of an annulus to obtain new results on super Fibonacci numbers.

CONTENTS

Introduction	1
1. Background on Decorated Super Teichmüller Theory	2
2. Super-Matrices and $\mathrm{OSp}(1 2)$	5
3. A Flat $\mathrm{OSp}(1 2)$ -Connection	6
4. Proof of Theorem 3.10	10
5. Double Dimer Interpretation of Matrix Formulae	21
6. Super Fibonacci Numbers Revisited	30
7. Geometric Interpretation	33
Acknowledgments	37
References	38

Introduction

Cluster algebras, first introduced by Fomin and Zelevinsky [FZ02], are certain commutative algebras possessing additional combinatorial structures. Since their discovery, cluster algebras have been connected to many other areas of mathematics and physics such as representation theory, integrable systems, Teichmüller theory and string theory. In recent years, much progress have been made towards a theory of super-commutative cluster algebras, such as [Ovs15, OS19], [LMRS21], [SV22, She22] and [MOZ21, MOZ22]. The current authors, in our previous two papers [MOZ21, MOZ22], began the project of exploring a possible super cluster algebraic interpretation of Penner-Zeitlin's decorated super Teichmüller theory, generalizing the known cluster structure of Penner's λ -length coordinates. This paper is the third in this series, and as such we will use several conventions and definitions from our previous works, citing them where appropriate.

School of Mathematics, University of Minnesota, Minneapolis, MN 55455, USA.

Email: musiker@umn.edu, ovenh001@umn.edu, swzhang@umn.edu.

For a triangulation T of a marked surface (S, M) , we define a graph Γ_T embedded in S and for each point of the decorated super Teichmüller space, a flat $\mathrm{OSp}(1|2)$ -connection on Γ_T . A similar construction was given in [Bou13] of a graph connection in terms of shear coordinates on the (un-decorated) super Teichmüller space¹. We then define certain canonical paths on Γ_T for each arc (a, b) of S , thereby associating the arc with a holonomy matrix $H_{a,b}$. Our main result (Theorem 3.10) is that for a polygon (i.e. a marked disk) the $(1, 2)$ -entry of the holonomy matrix is the super λ -length, up to sign. We also give precise formulas for all entries of the holonomy matrices in terms of super λ -lengths and μ -invariants (Theorem 4.3), and we give combinatorial interpretations of these matrix entries (Theorem 5.2) as generating functions for double dimer covers in the spirit of [MW13].

The structure of the paper is as follows. In Section 1, we review background on the decorated super Teichmüller theory of [PZ19], and recall some conventions in our previous papers [MOZ21, MOZ22]. In Section 2, we provide necessary information on super-matrices and the ortho-symplectic group $\mathrm{OSp}(1|2)$. In Section 3, we define the graph Γ_T and a flat $\mathrm{OSp}(1|2)$ -connection on it, and state our main theorem. A more detailed version of our matrix formulas can be found in Section 4 which is devoted to a proof of the main theorem. In Section 5 we give a combinatorial interpretation of the result of this paper using double dimer covers, connecting the main results of the current paper and those of [MOZ22]. We revisit the *super Fibonacci numbers* studied in [MOZ22], and examine the corresponding holonomy matrices in Section 6. Finally, in Section 7, we provide a more geometric interpretation of our matrix formula, via a different viewpoint of the decorated super Teichmüller theory.

1. Background on Decorated Super Teichmüller Theory

In this section, we briefly recall the basic definitions of the decorated super Teichmüller space of a polygon (see [PZ19] and [MOZ21] for more details). Consider a polygon P (i.e. a disc with marked points on its boundary), a fixed triangulation T , and a choice of orientation of the edges of T .

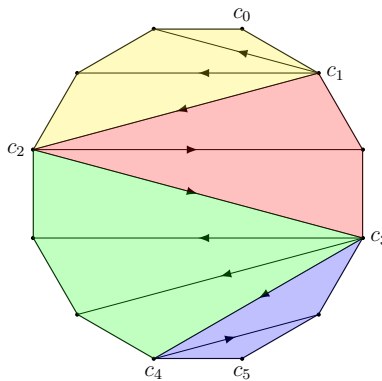


FIGURE 1. The default orientation of a generic triangulation where each fan segment is colored differently.

¹In the language of the cluster algebra literature, shear coordinates are \mathcal{X} -type cluster variables, while λ -lengths are \mathcal{A} -type cluster variables.

For simplicity, we will always consider a “*default orientation*”, as defined in [MOZ21], which is pictured in Figure 1. The maximal groupings of consecutive triangles which share a common vertex (indicated by different colors) are called “*fan segments*”, and the common vertex they share is called the “*fan center*” (vertices labelled c_1, c_2, \dots, c_N from top to bottom). The default orientation is defined so that the edges connecting fan centers are oriented $c_1 \rightarrow c_2 \rightarrow c_3 \rightarrow \dots \rightarrow c_N$, and the remaining edges are oriented *away* from the fan centers.

The *decorated super Teichmüller space* of P is a super-commutative algebra² \mathcal{A} with the following generators: for each edge in T with endpoints i and j , an even generator λ_{ij} (called a “ λ -length”), and for each triangle in T with vertices i, j, k , an odd generator \boxed{ijk} (called a “ μ -invariant”)³.

When two triangulations are related by a flip, as in Figure 2, one can define new elements of the algebra by the following “*super Ptolemy relations*”:

$$(1) \quad ef = ac + bd + \sqrt{abcd} \sigma \theta$$

$$(2) \quad \sigma' = \frac{\sigma \sqrt{bd} - \theta \sqrt{ac}}{\sqrt{ac + bd}} = \frac{\sigma \sqrt{bd} - \theta \sqrt{ac}}{\sqrt{ef}}$$

$$(3) \quad \theta' = \frac{\theta \sqrt{bd} + \sigma \sqrt{ac}}{\sqrt{ac + bd}} = \frac{\theta \sqrt{bd} + \sigma \sqrt{ac}}{\sqrt{ef}}$$

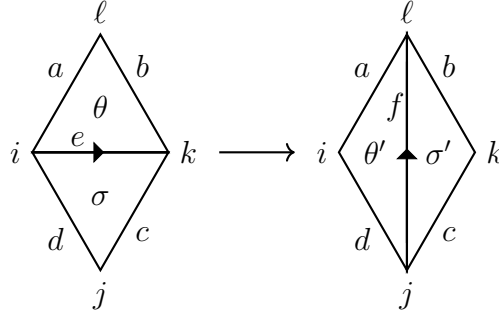


FIGURE 2. Super Ptolemy transformation

Note that in Equation (1), the order of multiplying the two odd variables σ and θ is determined by the orientation of the edge being flipped (see the arrow in Figure 2).

In Figure 2, the orientations of the four boundary edges are omitted, but the super Ptolemy transformation does change the orientation of the edge labeled b (the edges a, c, d keep their same orientation).

Definition 1.1. For a triangle with vertices i, j, k , define the *h -length at vertex i* to be

$$h_{jk}^i = \frac{\lambda_{jk}}{\lambda_{ij} \lambda_{ik}}$$

²Technically, each choice of spin structure (represented by a choice of orientation of the triangulation) corresponds to a different connected component of the space.

³The algebra \mathcal{A} is technically the tensor product of the field of rational functions in the square roots of the λ -lengths and the exterior algebra generated by μ -invariants.

Note that this is the same as the definition of “ h -length” in the classical (i.e. non-super) case. See e.g. [Pen12].

Definition 1.2. For a triangle with vertices i, j, k and μ -invariant $\theta = \boxed{ijk}$, we also define two sets of *normalized μ -invariants*:

$$\begin{aligned} \Delta_{jk}^i &:= \sqrt{\frac{\lambda_{jk}}{\lambda_{ij}\lambda_{ik}}} \theta = \sqrt{h_{jk}^i} \theta, & \Delta_{ik}^j &:= \sqrt{\frac{\lambda_{ik}}{\lambda_{ij}\lambda_{jk}}} \theta = \sqrt{h_{ik}^j} \theta, & \Delta_{ij}^k &:= \sqrt{\frac{\lambda_{ij}}{\lambda_{ik}\lambda_{jk}}} \theta = \sqrt{h_{ij}^k} \theta, \\ \nabla_{jk}^i &:= \sqrt{\frac{\lambda_{ij}\lambda_{ik}}{\lambda_{jk}}} \theta = \sqrt{\frac{1}{h_{jk}^i}} \theta, & \nabla_{ik}^j &:= \sqrt{\frac{\lambda_{ij}\lambda_{jk}}{\lambda_{ik}}} \theta = \sqrt{\frac{1}{h_{ik}^j}} \theta, & \nabla_{ij}^k &:= \sqrt{\frac{\lambda_{ik}\lambda_{jk}}{\lambda_{ij}}} \theta = \sqrt{\frac{1}{h_{ij}^k}} \theta, \end{aligned}$$

all of which are associated to a (triangle, vertex) pair, i.e. to an angle.

Remark 1.3. The h -lengths and normalized μ -invariants within a triangle satisfy the following relations

$$\begin{aligned} (i) \quad h_{ik}^j &= \left(\frac{\lambda_{ik}}{\lambda_{jk}}\right)^2 h_{jk}^i & (iii) \quad \nabla_{ik}^j &= \frac{\lambda_{jk}}{\lambda_{ik}} \nabla_{jk}^i \\ (ii) \quad \Delta_{ik}^j &= \frac{\lambda_{ik}}{\lambda_{jk}} \Delta_{jk}^i & (iv) \quad \nabla_{ik}^j &= \lambda_{ij} \Delta_{jk}^i \end{aligned}$$

Remark 1.4. In terms of the normalized μ -invariants, the super Ptolemy relations (Equations (1) to (3)) take a very simple form. Using the labelling of vertices of the quadrilateral in Figure 2, we can rewrite these equations as follows.

$$\begin{aligned} (1^*) \quad \lambda_{j\ell} &= \frac{\lambda_{ij}\lambda_{kl} + \lambda_{il}\lambda_{jk}}{\lambda_{ik}} + \nabla_{ik}^j \nabla_{ik}^\ell \\ (2^*) \quad \Delta_{j\ell}^k &= \Delta_{ij}^k - \Delta_{il}^k \\ (3^*) \quad \Delta_{j\ell}^i &= \Delta_{jk}^i + \Delta_{k\ell}^i \end{aligned}$$

Proposition 1.5. *Let ijk and ikl be two adjacent triangles, with the edge separating the triangles oriented $i \rightarrow k$ (as in Figure 2). Then*

$$\begin{aligned} (a) \quad h_{j\ell}^i &= h_{jk}^i + h_{k\ell}^i + \Delta_{jk}^i \Delta_{k\ell}^i \\ (b) \quad h_{j\ell}^k &= h_{ji}^k + h_{il}^k + \Delta_{ji}^k \Delta_{il}^k \end{aligned}$$

Proof. We will just prove part (a). The calculation for (b) is analogous. By definition, $h_{j\ell}^i = \frac{\lambda_{j\ell}}{\lambda_{ij}\lambda_{il}}$. Using the super Ptolemy relation (Equation (1)) and substituting for $\lambda_{j\ell}$, we get

$$h_{j\ell}^i = \frac{\lambda_{ij}\lambda_{kl} + \lambda_{jk}\lambda_{il}}{\lambda_{ij}\lambda_{il}\lambda_{ik}} + \frac{\nabla_{ik}^j \nabla_{ik}^\ell}{\lambda_{ij}\lambda_{il}} = \frac{\lambda_{kl}}{\lambda_{il}\lambda_{ik}} + \frac{\lambda_{jk}}{\lambda_{ij}\lambda_{ik}} + \frac{\nabla_{ik}^j}{\lambda_{ij}} \cdot \frac{\nabla_{ik}^\ell}{\lambda_{il}}.$$

By definition, the first two terms are $h_{k\ell}^i$ and h_{jk}^i . By Remark 1.3(iv), the last term is equal to $\Delta_{jk}^i \Delta_{k\ell}^i$. \square

2. Super-Matrices and $\text{OSp}(1|2)$

An $m|n \times m|n$ (even) super-matrix M over a super-algebra can be written as a block matrix of the form

$$M = \left(\begin{array}{c|c} A & \Xi \\ \hline \Psi & B \end{array} \right),$$

where A, B are $m \times m, n \times n$ matrices with even entries, and Ψ, Ξ are $m \times n, n \times m$ matrices with odd entries. We follow the convention that Greek letters denote odd variables. The super-symmetric analogue of the determinant of a matrix, called *Berezinian*, is defined as follows.

$$\text{Ber}(M) := \det(B)^{-1} \det(A + \Xi B^{-1} \Psi)$$

when B is invertible. Let A^t denote the transpose of a matrix, the super-transpose of a super-matrix is defined as:

$$M^{\text{st}} := \left(\begin{array}{c|c} A^t & \Psi^t \\ \hline -\Xi^t & B^t \end{array} \right).$$

Consider the set of $2|1 \times 2|1$ super matrices over \mathcal{A} .

$$M = \left(\begin{array}{cc|c} a & b & \gamma \\ c & d & \delta \\ \hline \alpha & \beta & e \end{array} \right)$$

Its Berezinian is given by $\text{Ber}(M) = \frac{1}{e}(ad - bc) + \frac{\alpha}{e^2}(d\gamma - b\delta) + \frac{\beta}{e^2}(c\gamma - a\delta) - \frac{2\alpha\beta\gamma\delta}{e^3}$. Let J denote the following matrix

$$J = \left(\begin{array}{cc|c} 0 & 1 & 0 \\ -1 & 0 & 0 \\ \hline 0 & 0 & 1 \end{array} \right)$$

The group $\text{OSp}(1|2)$ is defined as the set of $2|1 \times 2|1$ super-matrices g with $\text{Ber}(g) = 1$, and satisfying $g^{\text{st}} J g = J$. These constraints can be written down explicitly in the following system of equations.

$$(4) \quad e = 1 + \alpha\beta$$

$$(5) \quad e^{-1} = ad - bc$$

$$(6) \quad \alpha = c\gamma - a\delta$$

$$(7) \quad \beta = d\gamma - b\delta$$

$$(8) \quad \gamma = a\beta - b\alpha$$

$$(9) \quad \delta = c\beta - d\alpha$$

Notice that combining equations (4) and (5) gives us that

$$(10) \quad ad - bc = 1 - \alpha\beta.$$

Cross multiplying equations (6) and (8) or equations (7) and (9) gives us that

$$(11) \quad \alpha\beta = \gamma\delta.$$

Remark 2.1. Re-arranging the equation $g^{\text{st}}Jg = J$ gives $g^{-1} = J^{-1}g^{\text{st}}J$. Thus if $\text{Ber}(g) = 1$, then $g \in \text{OSp}(1|2)$ if and only if the inverse is given by

$$g^{-1} = \left(\begin{array}{cc|c} a & b & \gamma \\ c & d & \delta \\ \hline \alpha & \beta & e \end{array} \right)^{-1} = \left(\begin{array}{cc|c} d & -b & -\beta \\ -c & a & \alpha \\ \hline \delta & -\gamma & e \end{array} \right)$$

Now we define special elements of $\text{OSp}(1|2)$ which will be the main ingredients in our matrix formulas in Section 3.

Definition 2.2. Let x and h be even variables (with \sqrt{h} well-defined), and θ an odd variable. Then we define the following matrices:

$$E(x) = \left(\begin{array}{cc|c} 0 & -x & 0 \\ 1/x & 0 & 0 \\ \hline 0 & 0 & 1 \end{array} \right) \quad A(h|\theta) = \left(\begin{array}{cc|c} 1 & 0 & 0 \\ h & 1 & -\sqrt{h}\theta \\ \hline \sqrt{h}\theta & 0 & 1 \end{array} \right) \quad \rho = \left(\begin{array}{cc|c} -1 & 0 & 0 \\ 0 & -1 & 0 \\ \hline 0 & 0 & 1 \end{array} \right)$$

Their inverses are given by $\rho^{-1} = \rho$, $E(x)^{-1} = \rho E(x) = E(-x)$, and

$$A(h|\theta)^{-1} = \left(\begin{array}{cc|c} 1 & 0 & 0 \\ -h & 1 & \sqrt{h}\theta \\ \hline -\sqrt{h}\theta & 0 & 1 \end{array} \right)$$

If i, j, k are three marked points (vertices of a polyon), then we will almost always use the following shorthand notations:

$$E_{ij} := E(\lambda_{ij}) = \left(\begin{array}{cc|c} 0 & -\lambda_{ij} & 0 \\ \lambda_{ij}^{-1} & 0 & 0 \\ \hline 0 & 0 & 1 \end{array} \right) \quad A_{jk}^i := A\left(h_{jk}^i \left| \begin{array}{c} \boxed{ijk} \end{array} \right. \right) = \left(\begin{array}{cc|c} 1 & 0 & 0 \\ h_{jk}^i & 1 & -\Delta_{jk}^i \\ \hline \Delta_{jk}^i & 0 & 1 \end{array} \right)$$

Remark 2.3. The matrix ρ was called “fermionic reflection” in [PZ19]. Note that we have $\rho A(h|\theta)\rho = A(h|-\theta)$ (i.e. conjugation of A by ρ negates the fermionic variable θ). This is easy to see, since left-multiplication by ρ scales the first two rows by -1 , and right-multiplication by ρ scales the first two columns by -1 .

Remark 2.4. Observe that $\text{Ber } E(x) = \text{Ber } A(h|\theta) = \text{Ber } \rho = 1$, and that $A(h|\theta)^{-1}$, $E(x)^{-1}$, and ρ^{-1} have the form of Remark 2.1, and so these matrices are in $\text{OSp}(1|2)$.

3. A Flat $\text{OSp}(1|2)$ -Connection

Following [FG06, MW13], from a triangulation T of a marked surface with boundary, we will define a planar graph Γ_T and associate certain matrices to the (oriented) edges of the graph, giving a flat $\text{OSp}(1|2)$ -connection.

Remark 3.1. Although our main results (Theorem 3.10 and Theorem 4.3) are stated only for polygons, the constructions given below for Γ_T and the connection make sense for any triangulated surface. For a surface with non-trivial topology, the monodromy of this connection should coincide (up to conjugation) with the representation $\pi_1(S) \rightarrow \mathrm{OSp}(1|2)$ described in section 6 of [PZ19]. The benefit of our approach is that we are able to get nontrivial information even in the case of a polygon (where the fundamental group is trivial).

Definition 3.2. Inside each triangle of T , there is a hexagonal face of Γ_T with three sides parallel to the sides of the triangle. When two triangles share a side, the two vertices of Γ_T on opposite sides of this edge are connected (see Figure 3).

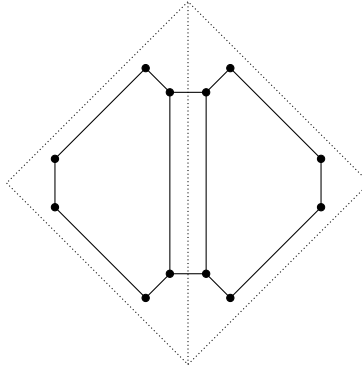


FIGURE 3. The graph Γ_T , with T in dashed lines.

Remark 3.3. The graph Γ_T has 3 kinds of edges and 2 kinds of faces. The three types of edges of Γ_T are:

- The edges parallel to arcs τ of the triangulation T . (If $\tau \in T$ is a boundary edge, then there is only one such edge of Γ_T , and if τ is an internal diagonal, then there are two such parallel edges in Γ_T .)
- The edges within a triangle that are *not* parallel to arcs τ of T . (These naturally correspond to the angles of the triangles.)
- The edges which cross the arcs τ of T .

The two types of faces are as follows:

- Within each triangle of T , there is a hexagonal face of Γ_T .
- Surrounding each internal diagonal of T , there is a quadrilateral face of Γ_T .

Definition 3.4. For a graph embedded on a surface, a *graph connection* is an assignment of a matrix to each oriented edge, such that opposite orientations of the same edge are assigned inverse matrices. For a path in the graph, the *holonomy* is the corresponding composition/product of matrices along the path. If the path is a loop, then the holonomy is also called *monodromy*. A connection is called *flat* if the monodromy around each contractible face is the identity matrix.

We will now define a flat $\mathrm{OSp}(1|2)$ -connection on the graph Γ_T .

Definition 3.5. Given (S, M) and T with a given orientation, we define the following holonomy matrices for the edges described in Remark 3.3. They are pictured in Figure 4.

- (1) Inside triangle ijk , the clockwise orientation of the edge at angle i is assigned the matrix $A(h_{jk}^i|\theta)$.
- (2) Inside triangle ijk , the clockwise orientation of the edge ij is assigned the matrix $E(\lambda_{ij})$.
- (3) For each internal diagonal ij , there are two edges of Γ_T which cross ij . Supposing that the spin structure has orientation $i \rightarrow j$, the edge closer to i is assigned the identity matrix, and the edge closer to j is assigned ρ (the fermionic reflection).

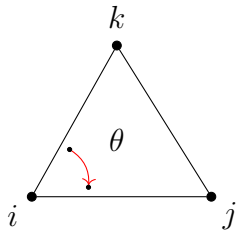
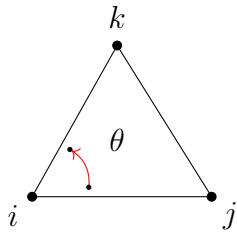
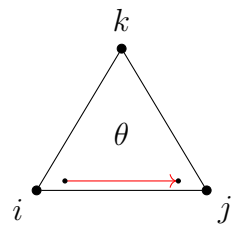
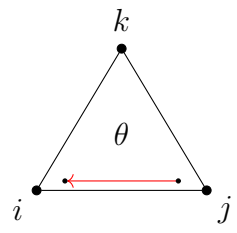
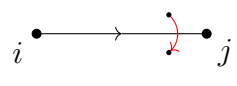
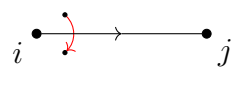
Type (i)		$A_{jk}^i{}^{-1}$		A_{jk}^i
Type (ii)		E_{ij}^{-1}		E_{ij}
Type (iii)		ρ		id

FIGURE 4. The three types of holonomy matrices.

Proposition 3.6. *The holonomy matrices from Definition 3.5 define a flat $\text{OSp}(1|2)$ -connection on Γ_T .*

Proof. As was mentioned in Remark 3.3, there are only two types of faces in Γ_T . So we only need to check that these two types of monodromy give the identity matrix. Also note that changing the starting point of a cycle changes the monodromy only by conjugation. So if we verify that a particular monodromy around a face is the identity, then the same follows for any starting point.

First let us consider a rectangular face corresponding to a diagonal ij of the triangulation. The (counter-clockwise) monodromy around this face is

$$\text{id} \cdot E_{ij} \cdot \rho \cdot E_{ij}$$

But since $\rho \cdot E_{ij} = E_{ij}^{-1}$, this gives the result.

Second, we must consider a hexagonal face inside a triangle ijk . The (clockwise) monodromy around this face, starting near vertex i , is given by

$$A_{jk}^i E_{ji} A_{ik}^j E_{kj} A_{ij}^k E_{ik}$$

It is straightforward to check that this product is the identity matrix. \square

Remark 3.7. Since the connection is flat, the holonomy between two vertices of Γ_T does not depend on the choice of path, since the graph is planar and any two paths are homotopic (thought of as paths on the ambient surface).

Remark 3.8. Note that the additional data of the spin structure on the triangulation T allows an additional elementary step corresponding to ρ that was not present in [FG06] nor [MW13]. However, its inclusion ensures that all monodromies yield the identity matrix (rather than the identity matrix up to sign).

Definition 3.9. If vertex i of a polygon is incident to m triangles in T , then there are $2m$ vertices of Γ_T corresponding to the angles of these triangles at m . We will say that any of these $2m$ vertices of Γ_T are “near” the vertex m .

Theorem 3.10. *Suppose we have a triangulation T of a polygon endowed with an orientation. Let i and j be two vertices of the polygon, and i' and j' any vertices of Γ_T that are near i and j , and let H be the holonomy from i' to j' . Then the $(1,2)$ -entry of H is equal to $\pm\lambda_{ij}$.*

We will prove this theorem in the next section. The first step in partially proving this theorem is the following.

Lemma 3.11. *The result of Theorem 3.10 does not depend on the particular choices of i' and j' .*

Proof. Choosing different i' or j' near the same i and j corresponds to multiplying H (on the right for i and the left for j) by a product of matrices of the following types: A_{jk}^i , A_{jk}^{i-1} , ρ , or id . Note that we do not need a separate case for ρ^{-1} since $\rho^{-1} = \rho$. See Figure 5 for an illustration of the different cases. In the figure, adding the red edge to the beginning of the blue path corresponds to prepending (i.e. right-multiplying) the holonomy by the indicated matrix.

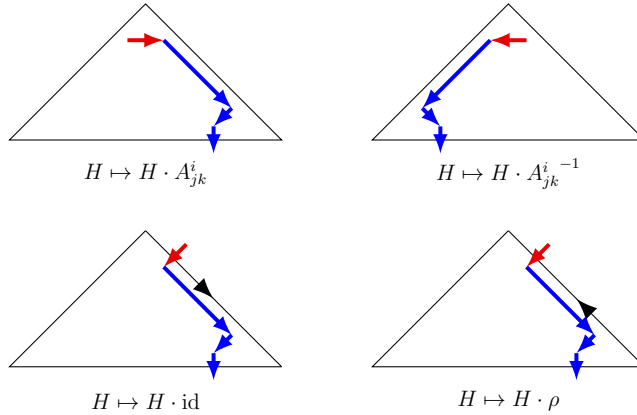


FIGURE 5. The different ways to move to another “near” vertex.

In the third case, multiplying by ρ (on either the left or right) will negate the $(1,2)$ -entry. For the first and second case, it is easy to see (simply by matrix multiplication) that multiplying on the left or right by A_{jk}^i or A_{jk}^{i-1} will not change the $(1,2)$ -entry. \square

4. Proof of Theorem 3.10

This section is devoted to a proof of our main theorem, Theorem 3.10. We first state a more detailed version of the main theorem. Let T be a generic triangulation with default orientation, and with fan centers labelled as c_i for $1 \leq i \leq N$. Let (a, b) be the longest diagonal in T and denote $a = c_0$ and $b = c_{N+1}$.

Definition 4.1. Let $H_{a,b}$ denote the holonomy following a path from a vertex near $a = c_0$ (on the side closer to c_1) to a vertex near $b = c_{N+1}$ (on the side closer to c_N). We say that the holonomy is of type $\epsilon_a \epsilon_b$ where

$$\epsilon_a = \begin{cases} 0 & \text{if } (c_0, c_1, c_2) \text{ are oriented clockwise,} \\ 1 & \text{otherwise.} \end{cases}$$

$$\epsilon_b = \begin{cases} 0 & \text{if } (c_{N-1}, c_N, c_{N+1}) \text{ are oriented clockwise,} \\ 1 & \text{otherwise.} \end{cases}$$

Remark 4.2. Note that given ϵ_a, ϵ_b is determined by the number of fans N via the relation $\epsilon_a + \epsilon_b = N + 1 \pmod{2}$.

Theorem 4.3. *Let T be a generic triangulation endowed with an arbitrary orientation (based on its spin structure), and with fan centers labelled as c_i for $1 \leq i \leq N$ and $a = c_0, b = c_{N+1}$. The holonomy matrix $H_{a,b}$ of type $\epsilon_a \epsilon_b$ is given by*

$$H_{a,b} = \left(\begin{array}{cc|c} -\frac{\lambda_{c_1, c_{N+1}}}{\lambda_{c_0, c_1}} & (-1)^{\epsilon_a} \lambda_{c_0, c_{N+1}} & \nabla_{c_0, c_1}^{c_{N+1}} \\ (-1)^{\epsilon_b} \frac{\lambda_{c_1, c_N}}{\lambda_{c_0, c_1} \lambda_{c_N, c_{N+1}}} & (-1)^{\epsilon_a + \epsilon_b - 1} \frac{\lambda_{c_0, c_N}}{\lambda_{c_N, c_{N+1}}} & (-1)^{\epsilon_b - 1} \frac{1}{\lambda_{c_N, c_{N+1}}} \nabla_{c_0, c_1}^{c_N} \\ \hline \frac{1}{\lambda_{c_0, c_1}} \nabla_{c_N, c_{N+1}}^{c_1} & (-1)^{\epsilon_a - 1} \nabla_{c_N, c_{N+1}}^{c_0} & 1 + \star \end{array} \right)$$

Here the formula for the $(3, 3)$ -entry (i.e. $1 + \star$) can be given two equivalent ways, which (due to Remark 2.4) follows from applications of both Equation (4) and Equation (11):

$$1 + \star = 1 + (-1)^{\epsilon_a - 1} \frac{1}{\lambda_{c_0, c_1}} \nabla_{c_N, c_{N+1}}^{c_1} \nabla_{c_N, c_{N+1}}^{c_0} = 1 + (-1)^{\epsilon_b - 1} \frac{1}{\lambda_{c_N, c_{N+1}}} \nabla_{c_0, c_1}^{c_{N+1}} \nabla_{c_0, c_1}^{c_N}.$$

We begin the proof of Theorem 4.3 by considering the special case of a fan triangulation with default orientation. Without loss of generality, we will assume the fan has vertices labeled by $1, 2, \dots, n$ in cyclic order. In particular, there is one non-trivial fan center, but including the endpoints of the longest arc, we have $a = c_0 = 2, c_1 = 1$, and $b = c_2 = c_{N+1} = n$. We recover that the holonomy H_{2n} can only be type 00 or 11, see Figure 6.

4.1. Fan Triangulation. The next two results (Lemma 4.4 and Corollary 4.5) compute the holonomy of a path which stays near a fan center, and traverses over all the angles in a fan segment.

Lemma 4.4. *Suppose i, j, k, ℓ are vertices of a quadrilateral in counter-clockwise order, and the (oriented) triangulation contains the edge $i \rightarrow k$ (as in Figure 2). Then the product of A -matrices is*

$$(a) \ A_{k\ell}^i A_{jk}^i = A_{j\ell}^i$$

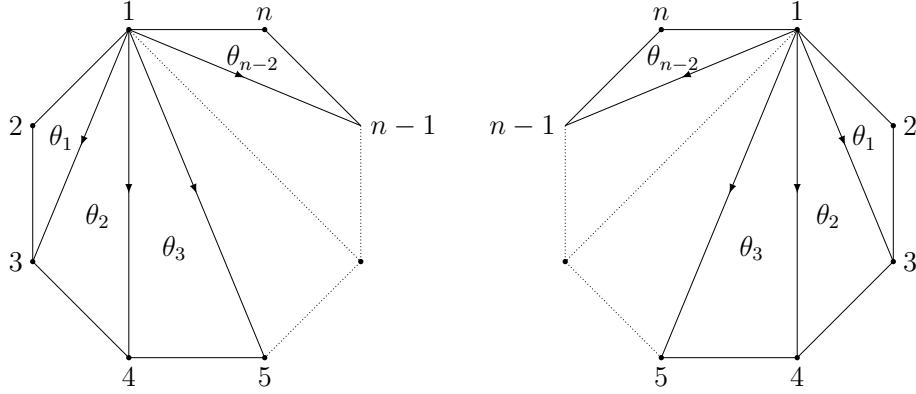


FIGURE 6. Single fan triangulation. Left: type 00. Right: type 11.

$$(b) A_{ij}^k \rho A_{il}^k = A_{jl}^k \rho$$

Proof. (a) Let $\theta = \boxed{ikl}$ and $\sigma = \boxed{ijk}$. The matrix product gives

$$\left(\begin{array}{cc|c} 1 & 0 & 0 \\ \hline h_{kl}^i + h_{jk}^i - \Delta_{kl}^i \Delta_{jk}^i & 1 & -\Delta_{jk}^i - \Delta_{kl}^i \\ \hline \Delta_{kl}^i + \Delta_{jk}^i & 0 & 1 \end{array} \right) = \left(\begin{array}{cc|c} 1 & 0 & 0 \\ \hline h_{jk}^i + h_{kl}^i + \Delta_{jk}^i \Delta_{kl}^i & 1 & -(\Delta_{jk}^i + \Delta_{kl}^i) \\ \hline \Delta_{jk}^i + \Delta_{kl}^i & 0 & 1 \end{array} \right).$$

By Proposition 1.5(a), the (2,1)-entry is equal to $h_{j\ell}^i$. By Equation (3*), the (2,3)- and (3,1)-entries are $-\Delta_{j\ell}^i$ and $\Delta_{j\ell}^i$, respectively.

(b) Recall from Remark 2.3 that $\rho A(h|\theta)\rho = A(h|\theta)$. By right-multiplying the equation in part (b) by ρ , the claim is equivalent to

$$A_{ij}^k A(h_{i\ell}^k | -\theta) = A_{jl}^k.$$

This matrix product is equal to

$$\left(\begin{array}{cc|c} 1 & 0 & 0 \\ \hline h_{ij}^k + h_{il}^k + \Delta_{ij}^k \Delta_{il}^k & 1 & \Delta_{il}^k - \Delta_{ij}^k \\ \hline \Delta_{ij}^k - \Delta_{il}^k & 0 & 1 \end{array} \right).$$

By Proposition 1.5(b) and Equation (2*), the (2,1)-entry is $h_{j\ell}^k$ and the (2,3)- and (3,1)-entries are $-\Delta_{j\ell}^k$ and $\Delta_{j\ell}^k$, respectively. \square

Corollary 4.5. *Consider a single fan triangulation with default orientation, as depicted in Figure 6. The ordered product of all A -matrices is*

$$(12) \quad A_{n-1,n}^1 \cdots A_{34}^1 A_{23}^1 = A_{2n}^1$$

if the holonomy is type 00, and

$$(13) \quad A_{n-1,n}^1{}^{-1} \cdots A_{34}^1{}^{-1} A_{23}^1{}^{-1} = A_{2n}^1{}^{-1}$$

if the holonomy is type 11.

Proof. This follows from Lemma 4.4 by induction. The base case of two triangles is simply Lemma 4.4. In general, if we first multiply the two right-most factors, they combine to give A_{24}^1 . After performing the associated flip on the arc $(1, 3)$, we now have a smaller polygon (on the vertices $1, 2, 4, 5, \dots, n-1, n$ in counter-clockwise order), again with a fan triangulation and the default orientation. For $k \geq 4$, after $(k-3)$ such steps, we have multiplied together the $(k-2)$ right-most factors into A_{2k}^1 and have flipped the arcs $(1, 3), (1, 4), \dots, (1, k-1)$ in order, resulting again in a smaller polygon, this time on the vertices $1, 2, k, k+1, \dots, n-1, n$, with a fan triangulation and the default orientation. So the result follows by induction. \square

The special case of Theorem 4.3 (and hence of Theorem 3.10) for a fan triangulation is the following.

Theorem 4.6. *Consider a fan triangulation with default orientation (as in Figure 6). The holonomy H_{2n} , of type $\epsilon\epsilon$, is given by*

$$H_{2n} = \left(\begin{array}{cc|c} -\frac{\lambda_{1n}}{\lambda_{12}} & (-1)^\epsilon \lambda_{2n} & \nabla_{12}^n \\ 0 & -\frac{\lambda_{12}}{\lambda_{1n}} & 0 \\ \hline 0 & -\nabla_{1n}^2 & 1 \end{array} \right)$$

In particular, the $(1, 2)$ -entry is equal to $\pm\lambda_{2n}$.

Proof. By Corollary 4.5, the holonomy is simply the product of three matrices:

$$E_{1n} A_{2n}^1 E_{12} \quad \text{or} \quad E_{1n}^{-1} A_{2n}^1 E_{12}^{-1}$$

After multiplying the matrices, use Remark 1.3 to simplify (in particular $\lambda_{1n} \Delta_{2n}^1 = \nabla_{12}^n$, and $-\lambda_{12} \Delta_{2n}^1 = -\nabla_{1n}^2$). \square

Remark 4.7. By Lemma 3.11, if we choose different starting and ending vertices near 2 and n , the resulting holonomy matrix will still have $(1, 2)$ -entry equal to $\pm\lambda_{2n}$.

4.2. Canonical paths. Given a generic triangulation T , we identify its fan centers as in Section 1, letting $a = c_0$ and $b = c_{N+1}$ so that (a, b) is the longest arc of T . We define two canonical paths along the corresponding graph Γ_T in order to compute the holonomy $H_{a,b}$ as follows.

The first one, called the *early-crossing canonical path* (or *early path* for short), is defined as follows:

- (1) For each $0 \leq k \leq N-1$, follow the E -edge parallel to (c_k, c_{k+1}) and then continue along a series of A -edges until reaching a point near (c_{k+1}, c_{k+2}) . Immediately cross the diagonal (c_{k+1}, c_{k+2}) .
- (2) Continue step (1) $N-1$ times until reaching the last fan segment. After crossing the diagonal (c_{N-1}, c_N) from a point near c_{N-1} , we follow by an E -edge parallel to (c_{N-1}, c_N) and continue along a series of A -edges until reaching a point near c_N as well as the arc (c_N, c_{N+1}) . We then end with the E -edge parallel to (c_N, c_{N+1}) .

We also define the *late-crossing canonical path* (or *late path* for short).

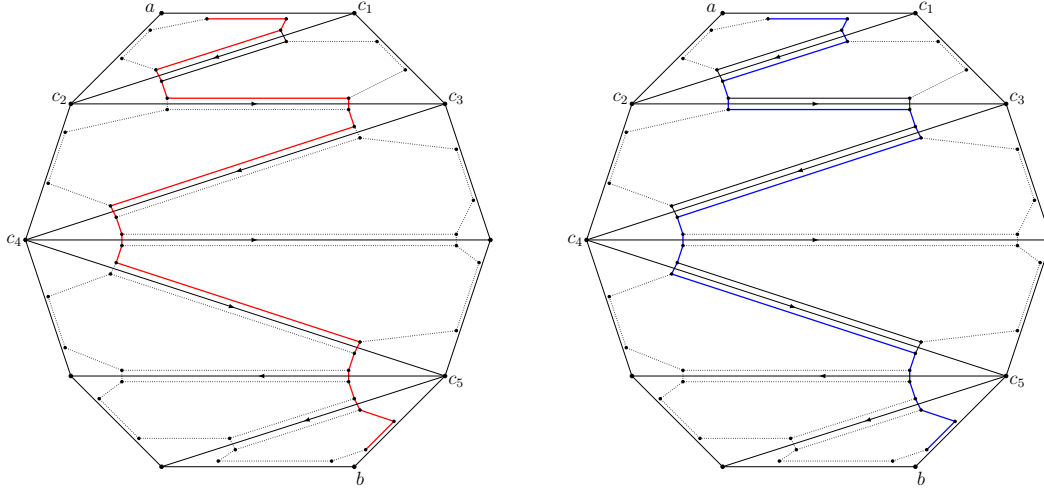


FIGURE 7. Left: Example of a late-crossing canonical path. Right: Example of an early-crossing canonical path (with default orientation illustrated).

- (1) Follow the E -edge parallel to (c_0, c_1) and then, as long as $N \geq 1$, continue along a series of A -edges until reaching a point near c_1 as well as the arc (c_1, c_2) . Immediately follow the E -edge parallel to (c_1, c_2) .
- (2) For $1 \leq k \leq N - 1$, cross the arc (c_k, c_{k+1}) , followed by A -edges until reaching a point near c_{k+1} as well as the arc (c_{k+1}, c_{k+2}) . Immediately follow the E -edge parallel to (c_{k+1}, c_{k+2}) .
- (3) After traversing along $N - 1$ such subpaths, we have arrived at a point near $b = c_{N+1}$.

Note that flipping the triangulation upside down turns an early path into a late path, and vice-versa.

4.3. Zig-Zag Triangulation. Let T be a zig-zag triangulation with default orientation, and with fan centers labelled as $c_i = i$, as depicted in Figure 8. Let $H_{a,b}$ denote the holonomy following one of the canonical paths from a vertex near $a = c_0$ (on the side closer to c_1) to a vertex near $b = c_{N+1}$ (on the side closer to c_N), as in Figure 7.

Remark 4.8. The holonomy matrix obtained from the late path will be a product of E , A , and ρ matrices. In particular, if we define $X_i := E_{i,i+1} A_{i-1,i+1}^i \rho$ and $Y_i := E_{i,i+1}^{-1} A_{i-1,i+1}^i \rho^{-1}$, then we will have the following forms for H_{ab} depending on the type⁴:

H_{ab}	$\epsilon_b = 0$	$\epsilon_b = 1$
$\epsilon_a = 0$	$X_N \cdots Y_4 X_3 Y_2 X_1 E_{01}^{-1}$	$Y_N \cdots Y_4 X_3 Y_2 X_1 E_{01}^{-1}$
$\epsilon_a = 1$	$X_N \cdots X_4 Y_3 X_2 Y_1 E_{01}$	$Y_N \cdots X_4 Y_3 X_2 Y_1 E_{01}$

⁴If $\epsilon_a = 0$, the late path actually starts $\cdots Y_2 E_{12} A_{02}^1 E_{01}$. But since $\rho^2 = \text{id}$ and $\rho E_{01} = E_{01}^{-1}$, this is equal to the more concise expression given in the table. Similarly when $\epsilon_a = 1$, the path starts with $\cdots X_2 E_{12}^{-1} A_{02}^1 E_{01}^{-1}$, but this is equal to the product shown.

To describe the early path, define $\mathcal{X}_i := A_{i-1,i+1}^i E_{i-1,i}$ and $\mathcal{Y}_i := A_{i-1,i+1}^{i-1} E_{i-1,i}^{-1}$. Then the early path will have the form

H_{ab}	$\epsilon_b = 0$	$\epsilon_b = 1$
$\epsilon_a = 0$	$E_{N,N+1} \mathcal{X}_N \cdots \mathcal{Y}_4 \mathcal{X}_3 \mathcal{Y}_2 \mathcal{X}_1$	$E_{N,N+1}^{-1} \mathcal{Y}_N \cdots \mathcal{Y}_4 \mathcal{X}_3 \mathcal{Y}_2 \mathcal{X}_1$
$\epsilon_a = 1$	$E_{N,N+1} \mathcal{X}_N \cdots \mathcal{X}_4 \mathcal{Y}_3 \mathcal{X}_2 \mathcal{Y}_1$	$E_{N,N+1}^{-1} \mathcal{Y}_N \cdots \mathcal{X}_4 \mathcal{Y}_3 \mathcal{X}_2 \mathcal{Y}_1$

Our proof has two parts: the first is an induction via left matrix multiplication, proving the first two columns of the holonomy matrix formula, and the second is an induction via right matrix multiplication, proving the formula for the first two rows. As mentioned earlier, the expression for the (3, 3)-entry follows immediately from Equation (4).

4.3.1. *Proof for the first two columns.* We first induct by left-multiplication, which corresponds to flipping certain diagonals from top to bottom. Recall that performing a quadrilateral flip will alter the orientation of another edge, so it is important that we keep track of the arrows as we perform a sequence of flips. For a zig-zag triangulation with default orientation $1 \rightarrow 2 \rightarrow \cdots \rightarrow N$, the natural flip sequence is from bottom to top⁵, because every flip in this sequence will not alter the arrows of other un-flipped edges. On the other hand, if we flip from top to bottom, certain steps in this sequence will change the orientation of other edges that are not yet flipped, which makes it difficult to keep track of the orientations. Therefore, we need to “manually” reverse all the arrows so that the top-to-bottom flip has the desired property.

It is explained in [PZ19] that reversing the arrows of a triangle and negating the μ -invariants is an equivalence of spin structure, so we start by applying this equivalence move on every even numbered triangles, i.e. c_{i-1}, c_i, c_{i+1} for even i . This will negate all the θ_i 's for even i and turn the orientation in to the reversed default orientation as desired. See Figure 8 for illustration.

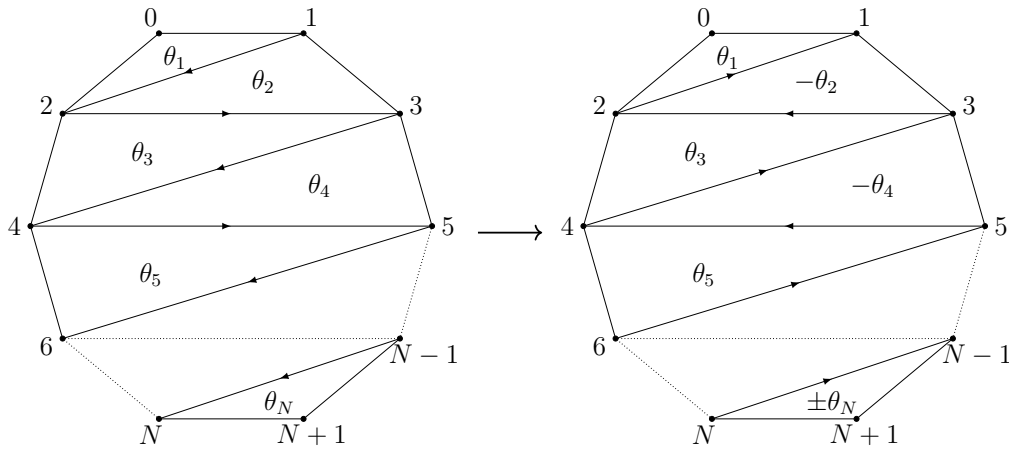


FIGURE 8. Reversing the default orientation of a zig-zag triangulation.

⁵This is called the *default flip sequence* in [MOZ21].

Proof. We show the proof of Theorem 4.3 only in the case when c_0, c_1, c_2 are oriented clockwise (i.e. $\epsilon_a = 0$), noting that the argument can be checked in a similar manner when $\epsilon_a = 1$. We will induct on N , the number of triangles.

Base Case. For the base case, we have a single triangle. In the notation from earlier in Section 4.3, we are computing H_{02} . Using Theorem 4.6 with the specialization $N = 1$ and using the labelling of Figure 6 (so that $c_0 = 2, c_1 = 1$, and $c_2 = 3$) yields the desired matrix $H_{a,b}$ after the proper substitutions, noting e.g. that λ_{ij} and \boxed{ijk} equals zero when $i = j$.

Next, when $k > 1$, we assume that the formula holds for $H_{0,k}$ and prove it for $H_{0,k+1}$. The induction step will be slightly different when k is even or odd. Note that if k is even (resp. odd), then the holonomy $H_{0,k}$ is of type 00 (resp. type 01) and $H_{0,k+1}$ is of type 01 (resp. type 00).

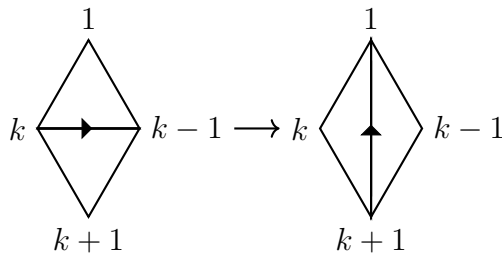
Inductive step for k even. By the induction hypothesis, we have

$$H_{0,k} = \left(\begin{array}{cc|c} -\frac{\lambda_{1k}}{\lambda_{01}} & \lambda_{0k} & \star \\ \frac{\lambda_{1,k-1}}{\lambda_{01}\lambda_{k-1,k}} & -\frac{\lambda_{0,k-1}}{\lambda_{k-1,k}} & \star \\ \hline \frac{1}{\lambda_{01}}\nabla_{k-1,k}^1 & -\nabla_{k-1,k}^0 & \star \end{array} \right)$$

Next we compute $H_{0,k+1} = Y_k H_{0,k} = E_{k,k+1}^{-1} A_{k-1,k+1}^k \rho H_{0,k}$:

$$(14) \quad \left(\begin{array}{cc|c} -\left(\frac{\lambda_{1,k}\lambda_{k-1,k+1} + \lambda_{1,k-1}\lambda_{k,k+1}}{\lambda_{0,1}\lambda_{k-1,k}} + \frac{\nabla_{k-1,k}^1 \nabla_{k-1,k}^{k+1}}{\lambda_{0,1}} \right) & \frac{\lambda_{0,k}\lambda_{k-1,k+1} + \lambda_{0,k-1}\lambda_{k,k+1}}{\lambda_{k-1,k}} - \nabla_{k-1,k}^{k+1} \nabla_{k-1,k}^0 & \star \\ \frac{\lambda_{1,k}}{\lambda_{01}\lambda_{k,k+1}} & \frac{\lambda_{0,k}}{\lambda_{k,k+1}} & \star \\ \hline \frac{\lambda_{1k}}{\lambda_{01}} (\Delta_{1,k-1}^k - \Delta_{k-1,k+1}^k) & \lambda_{0,k} (\Delta_{k-1,k+1}^k - \Delta_{0,k-1}^k) & \star \end{array} \right)$$

Note that the expressions in the first column are the Ptolemy relations (c.f. Remark 1.4) on the quadrilateral $(1, k, k-1, k+1)$. So matrix multiplication in the first column corresponds to flipping the edges $(2, 3), (3, 4), \dots, (k-1, k)$. Recall that the flips in this sequence will not alter the orientation of other (un-flipped) edges. So for every even k , the quadrilateral flip is depicted as follows, where the μ -invariants associated to the triangle $k-1, k, k+1$ are negated.

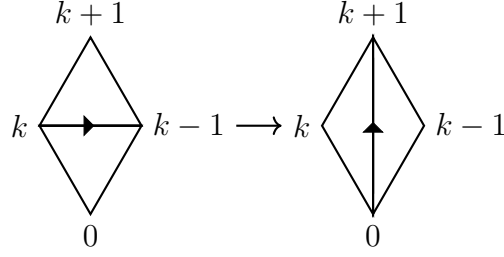


Thus by Equations (1*) and (2*), we have

$$\lambda_{1,k+1} = \frac{\lambda_{1,k}\lambda_{k-1,k+1} + \lambda_{1,k-1}\lambda_{k,k+1}}{\lambda_{k-1,k}} + (-\nabla_{k-1,k}^{k+1})\nabla_{k-1,k}^1$$

$$\Delta_{1,k+1}^k = (-\Delta_{k-1,k+1}^k) + \Delta_{1,k-1}^k$$

Now for the second column, the matrix multiplication corresponds to flipping the edges $(1, 2), (2, 3), \dots, (k-1, k)$. Similar to the previous case, the the quadrilateral flip is depicted as follows



and the Ptolemy relations are

$$\lambda_{0,k+1} = \frac{\lambda_{0,k}\lambda_{k-1,k+1} + \lambda_{0,k-1}\lambda_{k,k+1}}{\lambda_{k-1,k}} + (-\nabla_{k-1,k+1}^k)\nabla_{k-1,k}^0$$

$$\Delta_{0,k+1}^k = (-\Delta_{k-1,k+1}^k) + \Delta_{0,k-1}^k$$

Now plugging these back into Matrix (14), and using Remark 1.3 (iv) twice, we get

$$H_{0,k+1} = \left(\begin{array}{cc|c} -\frac{\lambda_{1,k+1}}{\lambda_{01}} & \lambda_{0,k+1} & \star \\ -\frac{\lambda_{1,k}}{\lambda_{01}\lambda_{k,k+1}} & \frac{\lambda_{0,k}}{\lambda_{k,k+1}} & \star \\ \hline \frac{\lambda_{1k}}{\lambda_{01}}\Delta_{1,k+1}^k & -\lambda_{0k}\Delta_{0,k+1}^k & \star \end{array} \right) = \left(\begin{array}{cc|c} -\frac{\lambda_{1,k+1}}{\lambda_{01}} & \lambda_{0,k+1} & \star \\ -\frac{\lambda_{1,k}}{\lambda_{01}\lambda_{k,k+1}} & \frac{\lambda_{0,k}}{\lambda_{k,k+1}} & \star \\ \hline \frac{1}{\lambda_{01}}\nabla_{k,k+1}^1 & -\nabla_{k,k+1}^0 & \star \end{array} \right).$$

This agrees with the formula of type 01 holonomy matrix.

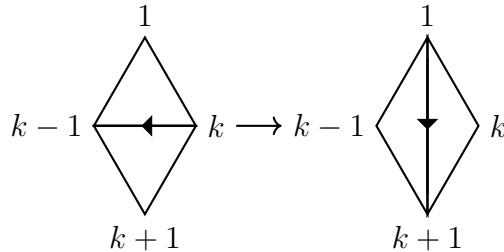
Induction step for k odd. By the induction hypothesis, we have

$$H_{0,k} = \left(\begin{array}{cc|c} -\frac{\lambda_{1,k}}{\lambda_{01}} & \lambda_{0,k} & \star \\ -\frac{\lambda_{1,k-1}}{\lambda_{01}\lambda_{k-1,k}} & \frac{\lambda_{0,k-1}}{\lambda_{k-1,k}} & \star \\ \hline \frac{1}{\lambda_{01}}\nabla_{k-1,k}^1 & -\nabla_{k-1,k}^0 & \star \end{array} \right)$$

Then we compute $H_{0,k+1} = X_k H_{0k} = E_{k,k+1} A_{k-1,k+1}^k \rho H_{0,k}$:

$$(15) \quad \left(\begin{array}{cc|c} -\left(\frac{\lambda_{1,k}\lambda_{k-1,k+1} + \lambda_{1,k-1}\lambda_{k,k+1}}{\lambda_{01}\lambda_{k-1,k}} + \frac{\nabla_{k-1,k}^1 \nabla_{k-1,k+1}^k}{\lambda_{01}}\right) & \frac{\lambda_{0,k}\lambda_{k-1,k+1} + \lambda_{0,k-1}\lambda_{k,k+1}}{\lambda_{k-1,k}} + \nabla_{k-1,k}^0 \nabla_{k-1,k+1}^k & \star \\ \frac{\lambda_{1,k}}{\lambda_{01}\lambda_{k,k+1}} & \frac{-\lambda_{0,k}}{\lambda_{k,k+1}} & \star \\ \hline \frac{\lambda_{1k}}{\lambda_{01}}(\Delta_{1,k-1}^k + \Delta_{k-1,k+1}^k) & -\lambda_{0k}(\Delta_{k-1,k+1}^k + \Delta_{0,k-1}^k) & \star \end{array} \right)$$

Similar to the k even case, the first column are Ptolemy relations corresponding to flipping the edges $(2, 3), (3, 4), \dots, (k-1, k)$. The last flip is depicted as follows. Note that in this case, the μ -invariant associated to the triangle $(k-1, k, k+1)$ is not negated.

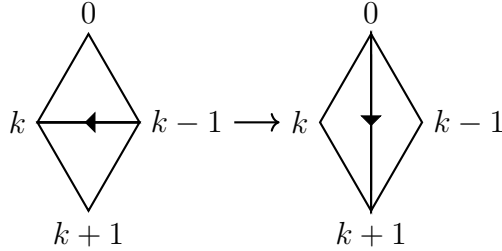


Thus by Equations (1*) and (3*), we have

$$\lambda_{1,k+1} = \frac{\lambda_{1,k}\lambda_{k-1,k+1} + \lambda_{1,k-1}\lambda_{k,k+1}}{\lambda_{k-1,k}} + \nabla_{k-1,k}^1 \nabla_{k-1,k}^{k+1}$$

$$\Delta_{1,k+1}^k = \Delta_{k-1,k+1}^k + \Delta_{1,k-1}^k$$

The matrix multiplication for the second column corresponds to flipping the edges, in order, $(1, 2), (2, 3), \dots, (k-1, k)$, where the the quadrilateral flip is depicted as follows



and the Ptolemy relations are

$$\lambda_{0,k+1} = \frac{\lambda_{0,k}\lambda_{k-1,k+1} + \lambda_{0,k-1}\lambda_{k,k+1}}{\lambda_{k-1,k}} + \nabla_{k-1,k}^0 \nabla_{k-1,k}^{k+1}$$

$$\Delta_{0,k+1}^k = \Delta_{k-1,k+1}^k + \Delta_{0,k-1}^k$$

Now plugging these Ptolemy relations into Matrix (15) we get

$$H_{0,k+1} = \left(\begin{array}{cc|c} -\frac{\lambda_{1,k+1}}{\lambda_{01}} & \lambda_{0,k+1} & \star \\ \frac{\lambda_{1,k}}{\lambda_{01}\lambda_{k,k+1}} & -\frac{\lambda_{0,k}}{\lambda_{k,k+1}} & \star \\ \hline \frac{\lambda_{1k}}{\lambda_{01}} \Delta_{1,k+1}^k & -\lambda_{0k} \Delta_{0,k+1}^k & \star \end{array} \right) = \left(\begin{array}{cc|c} -\frac{\lambda_{1,k+1}}{\lambda_{01}} & \lambda_{0,k+1} & \star \\ \frac{\lambda_{1,k}}{\lambda_{01}\lambda_{k,k+1}} & -\frac{\lambda_{0,k}}{\lambda_{k,k+1}} & \star \\ \hline \frac{1}{\lambda_{01}} \nabla_{k,k+1}^1 & -\nabla_{k,k+1}^0 & \star \end{array} \right)$$

This agrees with the formula of type 00 holonomy matrix. \square

4.3.2. *Proof for the first two rows.* Next we turn to the induction for the first two rows via right multiplication. In this case we will use the early path.

It turns out that induction by right multiplication corresponds to flipping the diagonals from bottom to top, as opposed to the previous case. This already has the property that each flip does not alter the orientation of other unflipped edges. Therefore here we do not need the extra step of reversing all the arrows.

Proof. We illustrate the proof in the case that c_{N-1}, c_N, c_{N+1} are oriented counterclockwise, i.e. the path is of type 01 or 11. In this case the holonomy matrix looks like

$$H_{0,N+1} = E_{N,N+1}^{-1} \mathcal{Y}_N \cdots \mathcal{Y}_2 \mathcal{X}_1 \quad \text{or} \quad E_{N,N+1}^{-1} \mathcal{Y}_N \cdots \mathcal{X}_2 \mathcal{Y}_1,$$

the former for type 01 and the latter for type 11 (recall that we are using the early path).

The base case is a triangle $H_{N-1,N+1} = E_{N,N+1}^{-1} A_{N-1,N+1}^N E_{N-1,N}$, which can be verified using Theorem 4.6 with the specialization $N = 1$.

We now assume by induction that the formula holds for $H_{k,N+1}$ for some $k < N$.

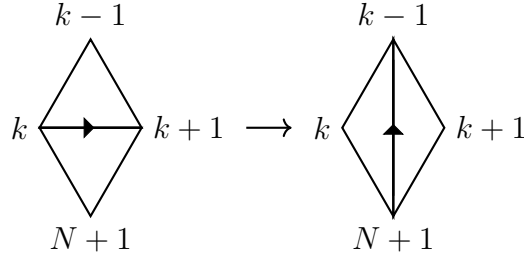
Induction step for $N - k$ even. If $N - k$ is even, i.e. there are even number of triangles in the sub-triangulation spanned by the diagonal $(k, N + 1)$, the holonomy $H_{k,N+1}$ is of type 01. Thus by induction hypothesis we have

$$H_{k,N+1} = \left(\begin{array}{cc|c} -\frac{\lambda_{k+1,N+1}}{\lambda_{k,k+1}} & \lambda_{k,N+1} & \nabla_{k,k+1}^{N+1} \\ -\frac{\lambda_{k+1,N}}{\lambda_{k,k+1}\lambda_{N,N+1}} & \frac{\lambda_{k,N}}{\lambda_{N,N+1}} & \frac{1}{\lambda_{N,N+1}}\nabla_{k,k+1}^N \\ \star & \star & \star \end{array} \right).$$

Then we compute $H_{k-1,N+1} = H_{k,N+1}\mathcal{Y}_k = H_{k,N+1}A_{k-1,k+1}^k E_{k-1,k}^{-1}$:

$$(16) \quad \left(\begin{array}{cc|c} -\frac{\lambda_{k,N+1}}{\lambda_{k-1,k}} & -\left(\frac{\lambda_{k-1,k}\lambda_{k+1,N+1} + \lambda_{k-1,k+1}\lambda_{k,N+1}}{\lambda_{k,k+1}} + \nabla_{k,k+1}^{N+1}\nabla_{k,k+1}^{k-1}\right) & \lambda_{k,N+1}(\Delta_{k+1,N+1}^k + \Delta_{k-1,k+1}^k) \\ -\frac{\lambda_{k,N}}{\lambda_{k-1,k}\lambda_{N,N+1}} & -\left(\frac{\lambda_{k-1,k}\lambda_{k+1,N} + \lambda_{k-1,k+1}\lambda_{k,N}}{\lambda_{k,k+1}\lambda_{N,N+1}} + \frac{\nabla_{k,k+1}^N\nabla_{k,k+1}^{k-1}}{\lambda_{N,N+1}}\right) & \frac{\lambda_{k,N}}{\lambda_{N,N+1}}(\Delta_{k+1,N}^k + \Delta_{k-1,k+1}^k) \\ \star & \star & \star \end{array} \right)$$

The expression on the first row are Ptolemy relations from flipping, starting from the bottom, the diagonals $(N, N + 1), (N - 1, N), \dots, (k, k + 1)$. The final flip in the sequence is depicted as follows:

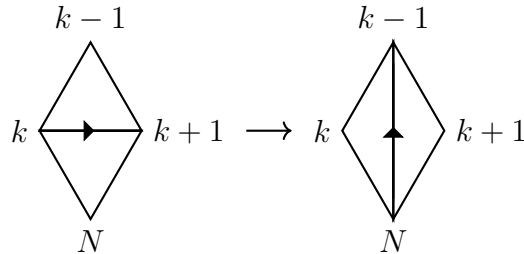


Equations (1*) and (3*) gives us

$$\lambda_{k-1,N+1} = \frac{\lambda_{k-1,k}\lambda_{k+1,N+1} + \lambda_{k-1,k+1}\lambda_{k,N+1}}{\lambda_{k,k+1}} + \nabla_{k,k+1}^{N+1}\nabla_{k,k+1}^{k-1}$$

$$\Delta_{k-1,N+1}^k = \Delta_{k-1,k+1}^k + \Delta_{k+1,N+1}^k$$

The expressions on the second row come analogously from flipping the diagonals $(N - 1, N), (N - 2, N - 1), \dots, (k, k + 1)$, where the final flip is depicted as follows.



Here the Ptolemy relations are

$$\lambda_{k-1,N} = \frac{\lambda_{k-1,k}\lambda_{k+1,N} + \lambda_{k-1,k+1}\lambda_{k,N}}{\lambda_{k,k+1}} + \nabla_{k,k+1}^N \nabla_{k,k+1}^{k-1}$$

$$\Delta_{k-1,N}^k = \Delta_{k-1,k+1}^k + \Delta_{k+1,N}^k$$

Now Plugging these relations into Equation (16), we get

$$H_{k-1,N+1} = \left(\begin{array}{cc|c} -\frac{\lambda_{k,N+1}}{\lambda_{k-1,k}} & -\lambda_{k-1,N+1} & \nabla_{k-1,k}^{N+1} \\ -\frac{\lambda_{k,N}}{\lambda_{k-1,k}\lambda_{N,N+1}} & -\frac{\lambda_{k-1,N}}{\lambda_{N,N+1}} & \frac{1}{\lambda_{N,N+1}} \nabla_{k-1,k}^N \\ \hline \star & \star & \star \end{array} \right)$$

which matches the formula for type 11 holonomy matrix.

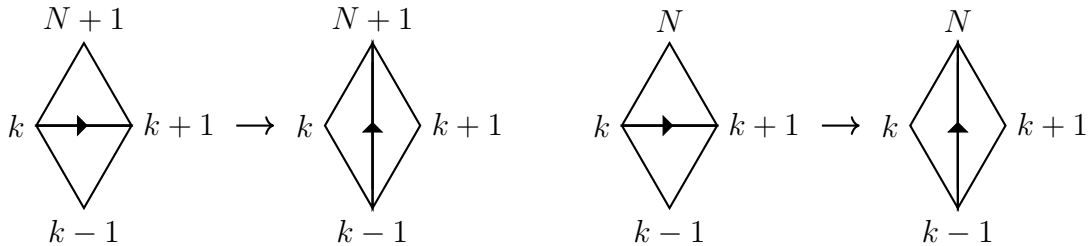
Induction step for $N - k$ odd. Next we turn to the case when $N - k$ is odd, where $H_{k,N+1}$ is of type 11 and $H_{k-1,N+1}$ is of type 01. By the induction hypothesis we have

$$H_{k,N+1} = \left(\begin{array}{cc|c} -\frac{\lambda_{k+1,N+1}}{\lambda_{k,k+1}} & -\lambda_{k,N+1} & \nabla_{k,k+1}^{N+1} \\ -\frac{\lambda_{k+1,N}}{\lambda_{k,k+1}\lambda_{N,N+1}} & -\frac{\lambda_{k,N}}{\lambda_{N,N+1}} & \frac{1}{\lambda_{N,N+1}} \nabla_{k,k+1}^N \\ \hline \star & \star & \star \end{array} \right)$$

Then we calculate $H_{k-1,N+1} = H_{k,N+1}X_k = H_{k,N+1}A_{k-1,k+1}^k E_{k-1,k}$:

$$(17) \quad \left(\begin{array}{cc|c} -\frac{\lambda_{k,N+1}}{\lambda_{k-1,k}} & \frac{\lambda_{k-1,k}\lambda_{k+1,N+1} + \lambda_{k-1,k+1}\lambda_{k,N+1}}{\lambda_{k,k+1}} + \nabla_{k,k+1}^{k-1} \nabla_{k,k+1}^{N+1} & \lambda_{k,N+1} (\Delta_{k+1,N+1}^k + \Delta_{k-1,k+1}^k) \\ -\frac{\lambda_{k,N}}{\lambda_{k-1,k}\lambda_{N,N+1}} & \frac{\lambda_{k-1,k}\lambda_{k+1,N} + \lambda_{k-1,k+1}\lambda_{k,N}}{\lambda_{k,k+1}\lambda_{N,N+1}} + \frac{\nabla_{k,k+1}^{k-1} \nabla_{k,k+1}^N}{\lambda_{N,N+1}} & \frac{\lambda_{k,N}}{\lambda_{N,N+1}} (\Delta_{k+1,N}^k + \Delta_{k-1,k+1}^k) \\ \hline \star & \star & \star \end{array} \right)$$

Similar to the previous case, the first row corresponds to the flip sequence given by the following $(N, N+1), (N-1, N), \dots, (k, k+1)$ and the second row corresponds to the flip sequence $(N-1, N), (N-2, N-1), \dots, (k, k+1)$, which are given by the following two diagrams respectively.



The Ptolemy relations are

$$\begin{aligned}\lambda_{k-1,N+1} &= \frac{\lambda_{k-1,k}\lambda_{k+1,N+1} + \lambda_{k-1,k+1}\lambda_{k,N+1}}{\lambda_{k,k+1}} + \nabla_{k,k+1}^{k-1} \nabla_{k,k+1}^{N+1} \\ \Delta_{k-1,N+1}^k &= \Delta_{k-1,k+1}^k + \Delta_{k+1,N+1}^k \\ \lambda_{k-1,N} &= \frac{\lambda_{k-1,k}\lambda_{k+1,N} + \lambda_{k-1,k+1}\lambda_{k,N}}{\lambda_{k,k+1}} + \nabla_{k,k+1}^{k-1} \nabla_{k,k+1}^N \\ \Delta_{k-1,N}^k &= \Delta_{k-1,k+1}^k + \Delta_{k+1,N}^k\end{aligned}$$

Plugging into Equation (17) we get

$$H_{k-1,N+1} = \left(\begin{array}{cc|c} -\frac{\lambda_{k,N+1}}{\lambda_{k-1,k}} & \lambda_{k-1,N+1} & \nabla_{k-1,k}^{N+1} \\ -\frac{\lambda_{k,N}}{\lambda_{k-1,k}\lambda_{N,N+1}} & \frac{\lambda_{k-1,N}}{\lambda_{N,N+1}} & \frac{1}{\lambda_{N,N+1}} \nabla_{k-1,k}^N \\ \star & \star & \star \end{array} \right)$$

which matches the formula for type 01 holonomy matrix.

We omit the proof of the other case when c_{N-1}, c_N, c_{N+1} are oriented clockwise. \square

Remark 4.9. In Section 4.3.2, it was noted that the matrix product computes the odd entries in the third column ($\nabla_{0,1}^{N+1}$ and $\frac{1}{\lambda_{N,N+1}} \nabla_{0,1}^N$) using a particular sequence of Ptolemy relations, which always uses Equation (3*), rather than Equation (2*), from Remark 1.4. Therefore by Theorem 6.2(b) from [MOZ22], these odd elements, when expressed as polynomials in the variables from the original triangulation, have all positive terms. Similarly, in Section 4.3.1, the matrix product computes the odd elements from the third row ($\frac{1}{\lambda_{01}} \nabla_{N,N+1}^1$ and $\nabla_{N,N+1}^0$) using Ptolemy relation Equation (2*), which can be seen as an instance of Equation (3*) after negating half of the odd variables, and reversing the orientations on all the diagonals. So although the polynomial expressions of these odd elements have some signs, Theorem 6.2(b) from [MOZ22] says that these expressions have all positive terms when expressed instead in the new variables $\theta'_i = (-1)^{i+1} \theta_i$.

We have now completed the proof of Theorem 4.3 (and hence of Theorem 3.10) for zig-zag triangulations with default orientation.

4.4. Generic Triangulation. The theorem for generic triangulations (with default orientation) is a direct consequence of the zig-zag case and Corollary 4.5. Write the holonomy as a product of matrices following one of the canonical paths. As we traverse through the i -th fan segment, we can use Corollary 4.5 to write the product of A -matrices in a fan as the single matrix $A_{c_{i-1}, c_{i+1}}^{c_i \pm 1}$. This is the same as flipping the diagonals inside each fan segment, which turns a generic triangulation into a zig-zag triangulation whose vertices are the original fan centers. See [MOZ21, Figure 15].

What remains is to consider the case of an orientation τ of T that is *not* the default one. In this case, it is possible to define the holonomy matrix $H_{a,b}$ as a product of matrices just as we did in Definition 3.5, but relative to orientation τ . The only difference will be that some instances of the matrix ρ will instead be an identity matrix, and vice-versa. The effect in either case is that the holonomy matrices crossing the edges whose orientation has changed are multiplied by ρ .

It is explained in [PZ19] (and again in [MOZ21, MOZ22] using our notations and conventions) that reversing the orientations around all three edges of a triangle corresponds to negating the associated odd variable. Also, it is possible to go from any orientation to the default one (the boundary edges may differ, but the interior diagonals can be made to agree with the default orientation) by a sequence of such orientation-reversals around triangles. So we may reduce the general case to examining what happens when we do this orientation-reversal in a single triangle.

When reversing the orientation of all three edges around a triangle, all six vertices of the hexagonal face of Γ_T in this triangle will be incident to an edge whose holonomy has been multiplied by ρ . If we perform a gauge transformation by ρ at each of these six vertices⁶, we can restore those edges to their previous weights (before we changed their orientations). Since each edge has two endpoints which are gauged, the effect on the three A matrices and the three E matrices will be that they are all conjugated by ρ . Since E commutes with ρ , and $\rho^2 = \text{id}$, this leaves the E -matrices unaffected. But as was pointed out in Remark 2.3, we have $\rho A(h|\theta)\rho = A(h|-\theta)$. So, in agreement with the remark in the preceding paragraph, the effect that this orientation-reversal has on the connection is simply to change $\theta \mapsto -\theta$ in the A -matrices.

It is clear that if a path passes through a vertex v of Γ_T , then a gauge transformation at v will not affect the holonomy along this path (the contributions of the incoming and outgoing edges will cancel). The conclusion here is that the holonomy formula from Theorem 4.3 still holds for arbitrary orientation, provided we negate the corresponding odd variables every time we do such an orientation-reversal around a triangle.

However, if the vertex v where we perform a gauge transformation is either the beginning or ending point of the path, then the holonomy *will* change. Specifically, if we reverse the orientations around the first or last triangle (or both), the effect on the holonomy is $H_{ab} \mapsto H_{ab}\rho$, or $H_{ab} \mapsto \rho H_{ab}$, or $H_{ab} \mapsto \rho H_{ab}\rho$.

5. Double Dimer Interpretation of Matrix Formulae

Motivated by the methods of Sections 4 and 5 of [MW13], we now provide a combinatorial interpretation of the holonomy matrices, which were defined in Section 3 and described explicitly for generic triangulations with the default orientation in Theorem 4.3. In the case considered in [MW13], the construction involved matrices in $\text{PSL}_2(\mathbb{C})$ whose entries were given interpretations in terms of perfect matchings of snake graphs. In the present work, we instead consider $2|1$ -by- $2|1$ matrices in the group $\text{OSp}(1|2)$, and obtain combinatorial interpretations of the entries in terms of double dimer covers of snake graphs, using results from [MOZ22].

Let T be an arbitrary acyclic triangulation of a polygon such that the arc (a, b) is the longest arc in T , i.e. it cuts through all internal arcs of T . Assume further that T is equipped with the default orientation with fan centers labeled as c_i for $1 \leq i \leq N$. Like in Section 4, we let $a = c_0$, $b = c_{N+1}$, and let H_{ab} be the holonomy as defined in Definition 4.1. The main result

⁶By a “gauge transformation by ρ at a vertex”, we mean left-multiplying all outgoing edge holonomies by ρ and right-multiplying all incoming edge holonomies by ρ .

of this section is to reinterpret the entries of $H_{a,b}$ as combinatorial generating functions as follows.

First, let \tilde{T} denote the triangulation that extends triangulation T by defining two new marked points, \tilde{a} and \tilde{b} , and adjoining the triangles (\tilde{a}, c_0, c_1) and $(c_N, c_{N+1}, \tilde{b})$, respectively about the edges (c_0, c_1) and (c_N, c_{N+1}) . We will use $\theta_{\tilde{a}}$ and $\theta_{\tilde{b}}$ to denote the μ -invariants associated to these two new triangles, respectively. See Figure 9. We let $\tilde{G} = G_{\tilde{T}}$ be the snake graph corresponding to the longest arc (\tilde{a}, \tilde{b}) in \tilde{T} , as defined initially in [MS10] and extended to the case of decorated super Teichmüller space in [MOZ22, Sec. 3].

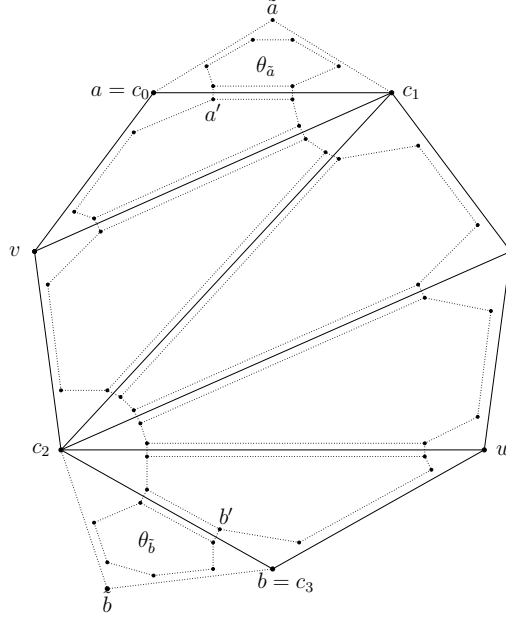


FIGURE 9. Extended triangulation \tilde{T} . We let v (resp. w) denote the fourth corner of the quadrilateral defined by the marked points \tilde{a} , $a = c_0$, and c_1 (resp. c_N , $b = c_{N+1}$, and \tilde{b}).

In \tilde{T} , we let i_1, i_2, \dots, i_d denote the internal arcs crossed in order by the longest arc (\tilde{a}, \tilde{b}) . In particular, $i_1 = (c_0, c_1)$ and $i_d = (c_N, c_{N+1})$.

Given our earlier definitions of ϵ_a and ϵ_b , and noting that in the quadrilateral on \tilde{a}, c_0, c_1, c_2 , the triangles (c_0, c_1, c_2) and (\tilde{a}, c_0, c_1) are of opposite orientations (and we have an analogous statement for the quadrilateral on $c_{N-1}, c_N, c_{N+1}, \tilde{b}$ we get the following equivalent usage of the values ϵ_a and ϵ_b :

$$\epsilon_a = \begin{cases} 0 & \text{if } (\tilde{a}, c_0, c_1) \text{ are oriented } \mathbf{counter}\text{-clockwise,} \\ 1 & \text{otherwise.} \end{cases}$$

$$\epsilon_b = \begin{cases} 0 & \text{if } (c_N, c_{N+1}, \tilde{b}) \text{ are oriented } \mathbf{counter}\text{-clockwise,} \\ 1 & \text{otherwise.} \end{cases}$$

When building the snake graph $G_{\tilde{T}}$, we note that as we progress from the bottom-left to the top right, the second tile is to the east (resp. north) of the first tile if $\epsilon_a = 0$ (resp. 1).

We use the following notation as shorthand for the weights that appear on the bottom and left edges of the first tile as well as the top and right edges of the last tile, in some order: $e_0 = \lambda_{\tilde{a}, e_0}$, $e_1 = \lambda_{\tilde{a}, e_1}$, $e_N = \lambda_{c_N, \tilde{b}}$, and $e_{N+1} = \lambda_{c_{N+1}, \tilde{b}}$. For example, e_0 is the weight of the bottom edge (resp. left edge) of the first tile if $\epsilon_a = 0$ (resp. $\epsilon_a = 1$), and e_1 is the weight of left edge (or bottom edge) respectively. See Figure 10. We will sometimes abuse notation and let e_0, e_1, e_N , and e_{N+1} denote the corresponding arcs themselves.

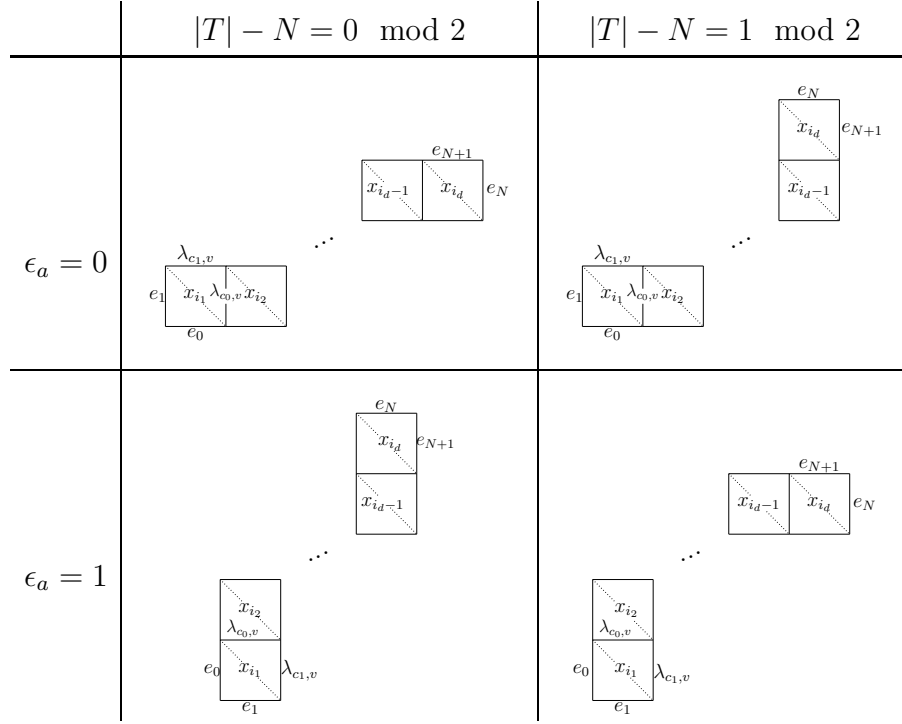


FIGURE 10. Different Snake Graphs as ϵ_a and $(|T| - N)$ vary, where $|T|$ is the number of triangles in T .

Definition 5.1. For a snake graph G , let $D(G)$ denote the set of double dimer covers of G . Also, let $D_{ab}(\tilde{G})$, $D^{cd}(\tilde{G})$, and $D_{ab}^{cd}(\tilde{G})$ denote the subsets of double dimer covers which includes (as sub-multisets) $\{e_a, e_b\}$, $\{e_c, e_d\}$, or $\{e_a, e_b, e_c, e_d\}$ respectively. Here, a and b will always be 0 or 1 (the bottom/left edges of the first tile), and c, d will always N or $N + 1$ (the top/right edges of the last tile).

Theorem 5.2. *The entries of $H_{a,b}$ each have combinatorial interpretations as weighted generating functions of double dimer covers of $G_{\tilde{T}}$, where each is subject to a restriction on the bottom-left and top-right tiles of $G_{\tilde{T}}$. More precisely $H_{a,b}$ is given by the following matrix:*

$$\frac{1}{x_{i_2} \cdots x_{i_{d-1}}} \left(\begin{array}{cc|c} \frac{1}{e_N} & 0 & 0 \\ 0 & \frac{(-1)^{\epsilon_b - 1}}{x_{i_d} e_{N+1}} & 0 \\ \hline 0 & 0 & \frac{1}{\sqrt{x_{i_d} e_N e_{N+1}}} \end{array} \right) \left(\begin{array}{cc|c} -\tilde{A} & -\tilde{B} & \tilde{\gamma} \\ -\tilde{C} & -\tilde{D} & \tilde{\delta} \\ \hline \tilde{\alpha} & \tilde{\beta} & \tilde{E} \end{array} \right) \left(\begin{array}{cc|c} \frac{1}{e_0 x_{i_1}} & 0 & 0 \\ 0 & \frac{(-1)^{\epsilon_a - 1}}{e_1} & 0 \\ \hline 0 & 0 & \frac{1}{\sqrt{e_0 e_1 x_{i_1}}} \end{array} \right)$$

such that

$$\tilde{A} = \sum_{M \in D_{00}^{NN}(\tilde{G})} \text{wt}(M), \quad \tilde{B} = \sum_{M \in D_{11}^{NN}(\tilde{G})} \text{wt}(M), \quad \tilde{\gamma} = \sum_{M \in D_{01}^{NN}(\tilde{G})} \text{wt}(M)^*$$

$$\begin{aligned}\tilde{C} &= \sum_{M \in D_{00}^{N+1, N+1}(\tilde{G})} \text{wt}(M), & \tilde{D} &= \sum_{M \in D_{11}^{N+1, N+1}(\tilde{G})} \text{wt}(M), & \tilde{\delta} &= \sum_{M \in D_{01}^{N+1, N+1}(\tilde{G})} \text{wt}(M)^* \\ \tilde{\alpha} &= \sum_{M \in D_{00}^{N, N+1}(\tilde{G})} \pm \text{wt}(M)^\dagger, & \tilde{\beta} &= \sum_{M \in D_{11}^{N, N+1}(\tilde{G})} \pm \text{wt}(M)^\dagger, & \tilde{E} &= \sum_{M \in D_{01}^{N, N+1}(\tilde{G})} \pm (\text{wt}(M)^*)^\dagger\end{aligned}$$

where $\text{wt}(M)$ denotes the weight of the double dimer cover (see [MOZ22, Def. 4.4]), and $(*)$ denotes the toggle operation on $\theta_{\tilde{a}}$ while (\dagger) indicates the toggle operation on $\theta_{\tilde{b}}$. In our cases, the toggle operation $(*)$ (resp. (\dagger)) removes $\theta_{\tilde{a}}$ (resp. $\theta_{\tilde{b}}$) from the corresponding term. See [MOZ22, Def. 5.6] for the more general definition.

The signs on the terms in $\tilde{\alpha}$ and $\tilde{\beta}$ are determined as in Remark 4.9. That is, $\text{wt}(M)$ is written in the positive order, followed by a substitution $\theta \mapsto -\theta$ for an appropriate subset of the odd variables (i.e. all those in the even-numbered fan segments). The \tilde{E} -entry also potentially contains terms of both signs, but it is more complicated to specify.

Note that even though the expression for H_{ab} in Theorem 5.2 involves the quantities e_0, e_1, e_N , and e_{N+1} , after reducing each of the nine matrix entries to lowest terms, such factors will always cancel. This is consistent with the fact that H_{ab} is defined by the arc (a, b) that is contained in the original triangulation T , where the triangles containing \tilde{a} and \tilde{b} do not appear.

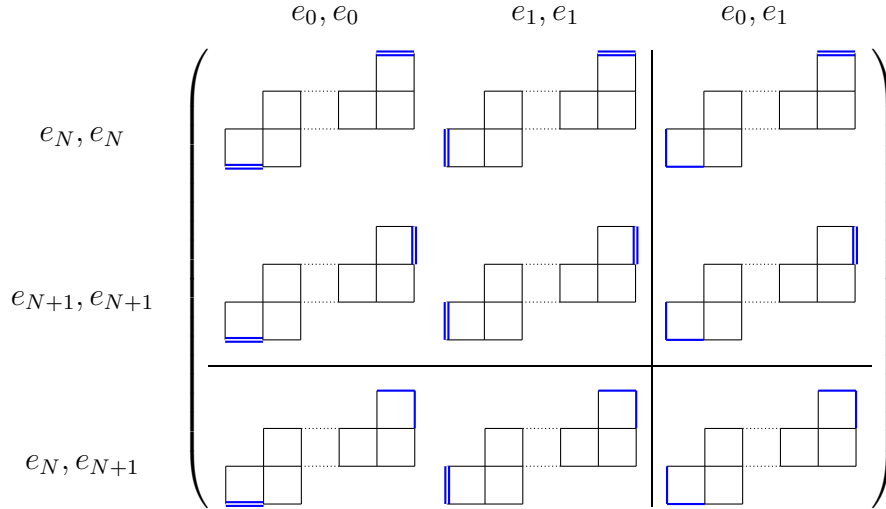


FIGURE 11. Graphical interpretations of entries of H_{ab} . Here the case of $\epsilon_a = 0$, $|T| - N = 1 \pmod{2}$ is illustrated.

Remark 5.3. Comparing the entries of the top-left 2-by-2 submatrix with the entries in the matrix appearing in Proposition 5.5 of [MW13], we see that our new result matches the expected formulas when we reduce to the classical case, up to using the identifications $x_a = e_0$, $x_b = e_1$, $x_w = e_N$ and $x_z = e_{N+1}$.

We now prove Theorem 5.2.

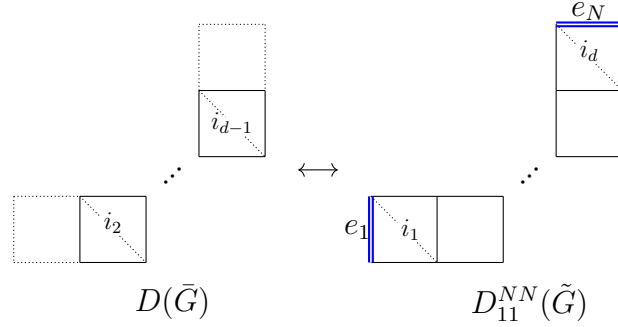


FIGURE 12. Illustrating part of the proof of Theorem 5.2 for the $(1, 2)$ -entry.

Proof. We begin with the $(1, 2)$ -entry of H_{ab} , namely $(-1)^{\epsilon_a} \lambda_{c_0, c_{N+1}}$. By Theorem 6.2(a) of [MOZ22], $\lambda_{c_0, c_{N+1}}$ can be expressed as the generating function counting double dimer covers in the snake graph G associated with the arc (c_0, c_{N+1}) :

$$\lambda_{c_0, c_{N+1}} = \frac{\sum_{M \in D(G)} \text{wt}(M)}{x_{i_2} \cdots x_{i_{d-1}}},$$

where $i_1, i_2, \dots, i_{d-1}, i_d$ label the arcs crossed by the arc (\tilde{a}, \tilde{b}) in order. In particular, arc (c_0, c_{N+1}) crosses the same list of arcs in order, except for $i_1 = (c_0, c_1)$ and $i_d = (c_N, c_{N+1})$. We have a bijection between $D(G)$ and $D_{11}^{NN}(\tilde{G})$ by appending a tile on either side of G (corresponding to arcs i_1 and i_d , respectively), and adjoining the doubled edges e_1 and e_N . See Figure 12. After dividing through by $e_1 e_N$, accounting for the weight of the doubled edges on the first and last tiles, it follows that $\lambda_{c_0, c_{N+1}} = \frac{\sum_{M \in D_{11}^{NN}(\tilde{G})} \text{wt}(M)}{(x_{i_2} \cdots x_{i_{d-1}}) e_1 e_N}$ as desired.

We next consider the $(2, 1)$ -entry of $H_{a,b}$, namely $(-1)^{\epsilon_b} \frac{\lambda_{c_1, c_N}}{\lambda_{c_0, c_1} \lambda_{c_N, c_{N+1}}}$. Assume that inside of the extended triangulation \tilde{T} , the fan center c_1 has $k \geq 2$ internal arcs incident to it, including the arcs $i_1 = (c_0, c_1)$ and $i_k = (c_1, c_2)$, while the fan center c_N has $\ell \geq 2$ internal arcs incident to it, including $i_{d-\ell+1} = (c_{N-1}, c_N)$ and $i_d = (c_N, c_{N+1})$. We let \bar{G} denote the snake graph associated to the arc (c_1, c_N) , noting that \bar{G} is a connected subgraph in the middle of G . Then, as above, Theorem 6.2(a) of [MOZ22] implies that λ_{c_1, c_N} equals $\frac{\sum_{M \in D(\bar{G})} \text{wt}(M)}{x_{i_{k+1}} \cdots x_{i_{d-\ell}}}$.

We have a bijection between $D(\bar{G})$ and $D_{00}^{N+1, N+1}(\tilde{G})$ by appending tiles on both sides of \bar{G} (corresponding to the zig-zag of tiles for arcs i_1, i_2, \dots, i_k on the one hand, and the zig-zag of tiles for arcs $i_{d-\ell+1}, \dots, i_{d-1}, i_d$ on the other), and adjoin the doubled edges e_0 and e_N on tiles i_1 and i_d , respectively. This leads to a cascade of doubled edges from both ends of \tilde{G} , giving a unique way to extend a given double dimer cover of \bar{G} . See Figure 13. We also divide through by $e_0 e_{N+1}$, as well as by $x_{i_2} x_{i_3} \cdots x_{i_k}$ and $x_{i_{d-\ell+1}} \cdots x_{i_{d-2}} x_{i_{d-1}}$ the latter of which account for the two cascades of doubled edges. Noting the equalities $(c_0, c_1) = i_1$ and $(c_N, c_{N+1}) = i_d$, it follows that $(-1)^{\epsilon_b} \frac{\lambda_{c_1, c_N}}{\lambda_{c_0, c_1} \lambda_{c_N, c_{N+1}}} = (-1)^{\epsilon_b} \frac{\sum_{M \in D_{00}^{N+1, N+1}(\tilde{G})} \text{wt}(M)}{(x_{i_1} \cdots x_{i_d}) e_0 e_{N+1}}$.

The proofs for the validity of the $(1, 1)$ - and $(2, 2)$ -entries are analogous and involve combinations of the previous two cases.

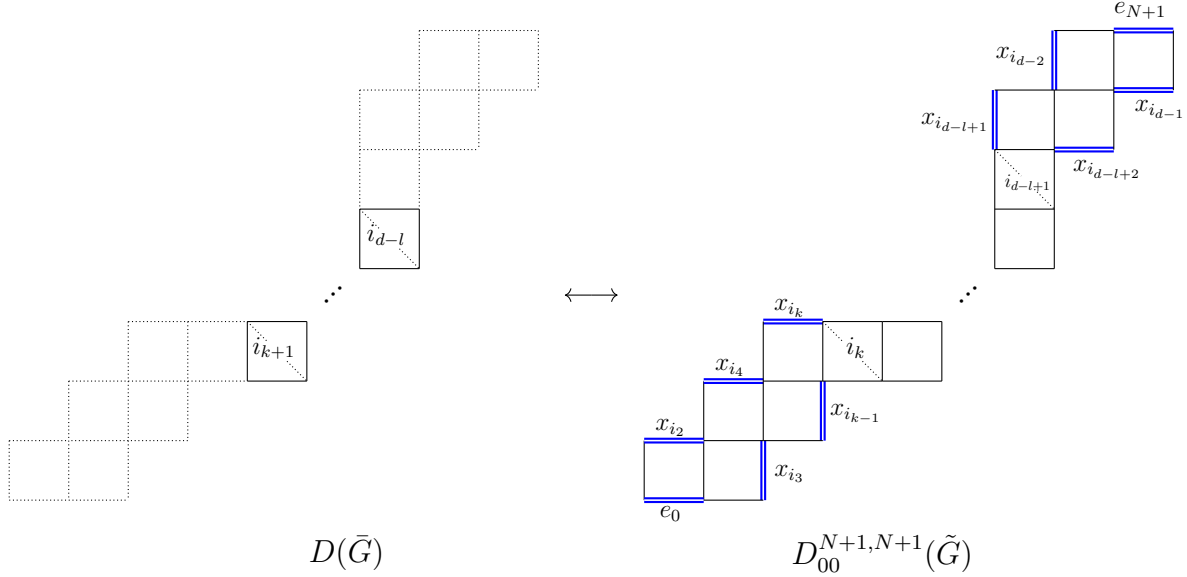


FIGURE 13. Illustrating part of the proof of Theorem 5.2 for the $(2, 1)$ -entry.

To prove the result for the $(1, 3)$ -, $(2, 3)$ -, $(3, 1)$ -, $(3, 2)$ -, and $(3, 3)$ -entries takes further work, and combining together Theorem 6.2(b) and Lemma 5.8, both of [MOZ22], as we now show:

Consider the $(1, 3)$ -entry of H_{ab} , namely $\nabla_{c_0, c_1}^{c_{N+1}} = \sqrt{\frac{\lambda_{c_0, c_{N+1}} \lambda_{c_1, c_{N+1}}}{\lambda_{c_0, c_1}}} \boxed{c_0, c_1, c_{N+1}}$.

We wish to apply Theorem 6.2(b) of [MOZ22] here to simplify this expression, but before we can do so we need to redraw the extended triangulation \tilde{T} so that it matches the illustration in Figure 13(a) of [MOZ22] so that $\boxed{c_0, c_1, c_{N+1}} = \varphi = \boxed{ijk}$. In particular, let v denote the endpoint of arc $i_2 = (c_1, v)$ so that the first two triangles of \tilde{T} are (\tilde{a}, c_0, c_1) and (c_0, c_1, v) respectively. Then in the notation of Figure 13(a) of [MOZ22], we have $a = (c_0, c_1)$, $b = (c_0, v)$, $d = (c_1, c_{N+1})$, $e = (c_1, v)$, and $f = (c_0, c_{N+1})$. If the first diagonal e is oriented incorrectly, we can reverse it and replace $\varphi \mapsto -\varphi$. As discussed in Remark 2.6 of [MOZ22], this does not change the positive ordering.

Theorem 6.2(b) of [MOZ22] then yields

$$\sqrt{\lambda_{c_1, c_{N+1}} \lambda_{c_0, c_{N+1}}} \boxed{c_0, c_1, c_{N+1}} = \frac{1}{x_{i_2} \cdots x_{i_{d-1}}} \sqrt{\frac{\lambda_{c_1, v}}{\lambda_{c_0, v}}} \sum_{M \in D_0(G)} \text{wt}(M)^{(*2)}$$

where G is the snake graph associated to the arc (c_0, c_{N+1}) (just as above) and $D_0(G) = D_{00}(G) \cup D_{01}(G)$ denotes the subset of double dimer covers that uses edge (c_0, v) as a single or doubled edge on the first tile of G .⁷

The notation $\text{wt}(M)^{(*2)}$ also signifies that the weight of the double dimer cover $M \in D_0(G)$ is altered by toggling $\boxed{c_0, c_1, v}$, the μ -invariant corresponding to the lower left triangle of the first tile of G (second tile of \tilde{G}).

⁷In [MOZ22], Theorem 6.2(b) uses the notations $D_t(G)$ and $D_r(G)$. The new notations used here allow a more uniform treatment.

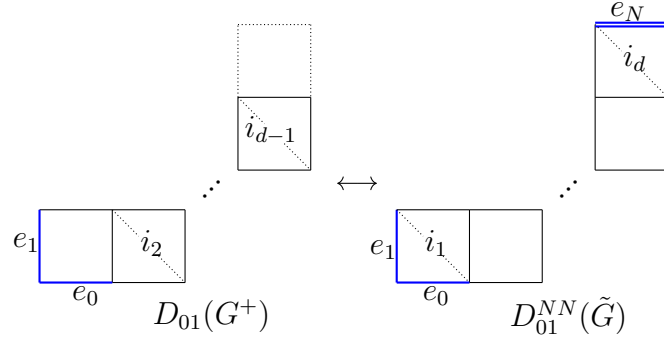


FIGURE 14. Illustrating part of the proof of Theorem 5.2 for the (1, 3)-entry.

By Lemma 5.8 of [MOZ22], there is a bijection between $D_0(G)$ and in $D_{01}(G^+)$ where G^+ is the subgraph of \tilde{G} that contains tiles i_1, i_2, \dots, i_{d-1} (i.e. it contains subgraph G plus tile i_1), where the weights are related by $\sum_{M \in D_0(G)} \text{wt}(M)^{(*2)} = \sqrt{\frac{\lambda_{c_0, v}}{e_0 e_1 \lambda_{c_1, v}}} \sum_{M \in D_{01}(G^+)} \text{wt}(M)^*$ where $(*2)$ toggles the weight by $\boxed{c_0, c_1, v}$ and $(*)$ toggles the weight by $\theta_{\tilde{a}} = \boxed{\tilde{a}, c_0, c_1}$.

The quantity $\sqrt{\frac{\lambda_{c_0, v}}{e_0 e_1 \lambda_{c_1, v}}}$ is based on the edge weights on the first tile, and recalling that arc $i_2 = (c_1, v)$.

Putting this altogether, and remembering that $\lambda_{c_0, c_1} = x_{i_1}$, we get

$$\sqrt{\frac{\lambda_{c_1, c_{N+1}} \lambda_{c_0, c_{N+1}}}{\lambda_{c_0, c_1}} \boxed{c_0, c_1, c_{N+1}}} = \frac{1}{\sqrt{x_{i_1}} (x_{i_2} \cdots x_{i_{d-1}})} \sqrt{\frac{\lambda_{c_1, v}}{\lambda_{c_0, v}}} \sqrt{\frac{\lambda_{c_0, v}}{e_0 e_1 \lambda_{c_1, v}}} \sum_{M \in D_{01}(G^+)} \text{wt}(M)^*.$$

Furthermore, there is another straightforward bijection between $D_{01}(G^+)$ and $D_{01}^{NN}(\tilde{G})$ by adjoining the last tile i_d , and utilizing the edge e_N as a double edge. See Figure 14. Dividing through by this contribution, and noting that the weight of the single forced edges on the first tile is $\sqrt{e_0 e_1}$, we thus conclude that the (1, 3)-entry of $H_{a, b}$ is

$$\frac{1}{\sqrt{e_0 e_1} \sqrt{x_{i_1}} (x_{i_2} \cdots x_{i_{d-1}}) e_N} \sum_{M \in D_{01}^{NN}(\tilde{G})} \text{wt}(M)^*$$

as desired.

We use an analogous argument to verify the formulas for the (2, 3)-, (3, 1)-, and (3, 2)-entries, noting that we must sometimes divide by $\lambda_{c_0, c_1} = x_{i_1}$ or $\lambda_{c_N, c_{N+1}} = x_{i_d}$ to get the formula. Also, as mentioned in Remark 4.9, the terms in \tilde{a} and $\tilde{\beta}$ will sometimes have signs. This is because Theorem 6.2(b) from [MOZ22] implicitly assumes one of two possible choices of positive ordering of the odd variables, and we need to use the opposite choice when applying the theorem to the (3, 1)- and (3, 2)-entries.

For the case of the (3, 3)-entry of $H_{a, b}$, we need to show that

$$1 + (-1)^{\epsilon_a - 1} \frac{1}{\lambda_{c_0, c_1}} \nabla_{c_N, c_{N+1}}^{c_1} \nabla_{c_N, c_{N+1}}^{c_0} = 1 + (-1)^{\epsilon_b - 1} \frac{1}{\lambda_{c_N, c_{N+1}}} \nabla_{c_0, c_1}^{c_{N+1}} \nabla_{c_0, c_1}^{c_N}$$

equals

$$\frac{1}{(x_{i_2} \cdots x_{i_{d-1}}) \sqrt{x_{i_1} x_{i_d}} \sqrt{e_0 e_1 e_N e_{N+1}}} \sum_{M \in D_{0,1}^{N,N+1}(\tilde{G})} (\text{wt}(M)^*)^\dagger.$$

Since we have already shown that the $(3, 1)$ - and $(3, 2)$ -entries each have the desired combinatorial interpretations, then by Equation (4), it remains to show that

$$\tilde{E} - \partial = \frac{(-1)^{\epsilon_a - 1}}{\partial} \tilde{\alpha} \tilde{\beta}$$

where $\partial := \sqrt{e_0 e_1 x_{i_1} (x_{i_2}^2 \cdots x_{i_{d-1}}^2) x_{i_d} e_N e_{N+1}}$ is the product of the (square roots of the) edge weights of all the outer boundary sides of \tilde{G} .

Note that among the double dimer covers in $D_{0,1}^{N,N+1}(\tilde{G})$, there is the unique one that consists of a single cycle comprised of the entire boundary of \tilde{G} . Based on the definition of edge weights on \tilde{G} , this will contribute to \tilde{E} a weight of $((\partial \theta_{\tilde{\alpha}} \theta_{\tilde{\beta}})^*)^\dagger = \partial$. This means the left-hand side, $\tilde{E} - \partial$, is simply the sum over $D_{0,1}^{N,N+1}$ minus this one special element.

Therefore, we need to show that

$$(-1)^{\epsilon_a - 1} \left(\sum_{M \in D_{00}^{N,N+1}} \text{wt}(M)^\dagger \right) \left(\sum_{M \in D_{11}^{N,N+1}} \text{wt}(M)^\dagger \right) = \text{wt}(M_0) \sum_{M \in D_{01}^{N,N+1} \setminus \{M_0\}} (\text{wt}(M)^*)^\dagger$$

where M_0 the special double dimer cover mentioned above (with weight $\text{wt}(M_0) = \partial$). We will do this by seeing that some pairs of terms in the product on the left-hand side cancel, and that the remaining terms are in bijection with the terms on the right-hand side, with weights differing by a factor of ∂ .

Let (M_1, M_2) be a pair of double dimer covers, where M_1 is in the $\tilde{\alpha}$ sum (over $D_{00}^{N,N+1}$) and M_2 is from the $\tilde{\beta}$ sum (over $D_{11}^{N,N+1}$). Let i_t denote the first internal (non-boundary) edge of \tilde{G} which is used in either M_1 or M_2 .

First consider the case when i_t is used as a double edge in either M_1 or M_2 . This is illustrated in Figure 15. Note that it cannot be used as a double edge in both because it is the *first* occurrence of an internal edge, and so at least one of the M_i 's uses an adjacent boundary edge twice. Let us assume (for simplicity of the following exposition) that i_t belongs to M_1 . In this case, the next two boundary edges adjacent to i_t (those immediately to the right or above) can be used by neither M_1 nor M_2 . Thus we can swap the portions of M_1 and M_2 to the right of i_t , and obtain a new pair (M'_1, M'_2) using the same edges. However, since we swapped the portions at the *end*, the odd variables corresponding to the cycles ending on the last tile now are multiplied in the opposite order. Therefore $\text{wt}(M_1)^\dagger \text{wt}(M_2)^\dagger + \text{wt}(M'_1)^\dagger \text{wt}(M'_2)^\dagger = 0$.

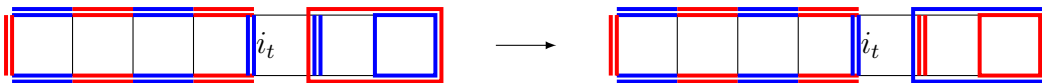


FIGURE 15. The case when i_t is a double edge. M_1 is in blue, and M_2 is in red.

In all the remaining terms, i_t is not used as a doubled edge, so it is used only once in either M_1 or M_2 . Note that if it is used as a single edge in both M_1 and M_2 then we would have

two cycles (one from M_1 and one from M_2) which contribute the same odd variable. But since $\theta^2 = 0$ for all odd variables, such terms would contribute a weight of zero. So we do not need to consider such configurations. So we only consider the case that i_t is used once in exactly one of the M_i 's (and is used either twice or not at all in the other). Again, assume for the sake of exposition that i_t is used only once in M_1 .

At this point we further divide into two cases: either the cycle of M_1 beginning at i_t continues until the last tile of \tilde{G} , or not.

Consider first the former case, which is pictured in Figure 16. Note that in the union $M_1 \cup M_2$, all boundary edges are used at least once. Indeed, all boundary edges before i_t are used twice, and all boundary edges after i_t are used in the cycle beginning at i_t . Therefore the product of the weights of M_1 and M_2 is divisible by ∂ , and what remains after deleting one instance of each boundary edge is a double dimer cover with at least two cycles: one starting at the first tile and ending at i_t , and one ending at the last tile of \tilde{G} (coming from M_2). This is precisely the type of configurations counted by $\tilde{E} - \partial$.



FIGURE 16. The case when i_t is part of a cycle going to the last tile (M_1 in blue, M_2 in red). Removing one copy of each boundary edge gives an element of \tilde{E} (in green).

In the latter case (when the cycle beginning at i_t does *not* extend all the way to the last tile of \tilde{G}), then let i_s be the internal edge which is either the top or right edge of the last tile of this cycle. We now consider the different cases by looking at the two boundary edges immediately to the right/above i_s . There are three cases, depending on if these boundary edges are used once, twice, or not at all by M_2 .

In the case that the boundary edges adjacent to i_s are not used at all in either M_1 or M_2 , then as described earlier (and pictured in Figure 15), we may swap the parts of M_1 and M_2 occurring after i_s to get another pair (M'_1, M'_2) whose product of weights cancels with (M_1, M_2) .

If these boundary edges are used twice by M_2 then replacing i_s with a double edge and looking at the truncated snake graph from i_s to the end, we are in the same situation we started with: the truncated M_1 has a double edge on one side of the first tile (either the left or bottom), and the truncated M_2 has a double edge on the other, while both still end with cycles. Therefore we may repeat the argument up to this point, looking for the next occurrence of an internal edge used by either M_1 or M_2 , and finding either another term that cancels, or concluding that this product $\frac{1}{\partial} \text{wt}(M_1)^\dagger \text{wt}(M_2)^\dagger$ represents a term from $\tilde{E} - \partial$.

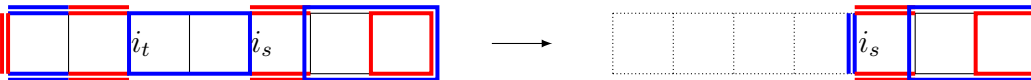


FIGURE 17. The case when i_t is part of a cycle that does *not* go to the last tile (M_1 in blue, M_2 in red). Removing the part of the picture before i_s results in a similar situation, in a smaller graph.

The final case that has not been considered is when M_2 uses the boundary sides adjacent to i_s once (not doubled). As mentioned before, M_2 cannot have a cycle beginning or ending adjacent to i_s (else the weight would be zero). Therefore we need only consider the case that M_2 has a cycle beginning before i_s and ending after i_s . Let $i_{s'}$ be the internal edge on the end of this cycle of M_2 . We continue the current argument with $i_{s'}$ instead of i_s . If $i_{s'}$ is not on the boundary of the last tile, we continue to look at the cases of the boundary sides adjacent to $i_{s'}$. Finally, if $i_{s'}$ is on the boundary of the last tile (which must eventually happen, since both M_1 and M_2 are assumed to end with cycles), then we are back in the earlier case and this gives a term from $\tilde{E} - \partial$.

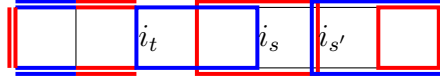


FIGURE 18. The case when the cycle starting at i_t overlaps with a cycle from M_2 (M_1 in blue, M_2 in red). We can continue the argument with $i_{s'}$ instead of i_s .

The inverse map, which shows that each term of $\tilde{E} - \partial$ can be written uniquely as the product of terms from α and β , can be constructed using an analysis similar to the above argument. \square

6. Super Fibonacci Numbers Revisited

In [MOZ22], we used the decorated super Teichmüller space of an annulus to find a sequence of λ -lengths satisfying a recurrence which generalizes the Fibonacci sequence. This is in the same spirit as Ovsienko’s “shadow sequences” [Ovs22], although our shadow of the Fibonacci sequence differs from his⁸.

In this section, we revisit these “super Fibonacci numbers” from the point of view of the matrix formulas presented in the current paper.

Consider an annulus with one marked point on each boundary component, and the oriented triangulation pictured in Figure 19, where all λ -lengths are equal to 1. Let z_n be λ -length of the arc connecting the two marked points which winds around the annulus $n - 2$ times. That is, $z_1 = z_2 = 1$ are the diagonals of the triangulation (in blue and red in Figure 19),

⁸Note that Ovsienko’s shadow sequence for the Fibonacci numbers actually coincides with the g_n ’s defined in [MOZ22, Sec. 11].

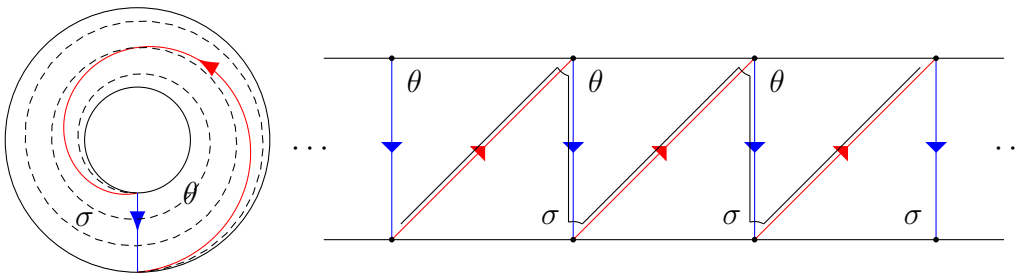


FIGURE 19. Left: Triangulation of an annulus. Right: its universal cover.

z_3 circles once, z_4 circles twice, etc. For example, z_4 is shown as a dashed line in the left picture of Figure 19. In [MOZ22], we showed that these satisfy the recurrence

$$z_n = (3 + 2\sigma\theta)z_{n-1} - z_{n-2} - \sigma\theta,$$

which generalizes a recurrence satisfied by the sequence of every-other Fibonacci number, i.e.

$$f_n = 3f_{n-2} - f_{n-4}$$

Furthermore, z_n ‘‘counts’’ double dimer configurations on the snake graph G_{2n-5} , which consists of a horizontal row of $2n - 5$ boxes. By this we mean z_n is the weight generating function of double dimer configurations, and since all even variables are set equal to 1, it is of the form $z_n = x_{2n-5} + y_{2n-5}\sigma\theta$, where x_k and y_k are integers. Specifically, $x_k = f_{k+1}$ counts those double dimer configurations on the horizontal strip of k boxes that are really single dimer covers (i.e. all edges are doubled), and y_k counts all double dimer configurations which contain one cycle surrounding an odd number of boxes⁹.

As in [MOZ22], let $w_n = x_{2n-4} + y_{2n-4}\sigma\theta$ be the corresponding generating function for double dimer covers on horizontal strips with an even number of boxes. These two sequences satisfy the following Fibonacci-like recurrences.

Lemma 6.1 ([MOZ22], Lemma 11.6). *The sequences z_n and w_n satisfy the following recurrences:*

$$\begin{aligned} (a) \quad z_n &= z_{n-1} + (1 + \sigma\theta)w_{n-1} \\ (b) \quad w_n &= w_{n-1} + (1 + \sigma\theta)z_n - \sigma\theta \end{aligned}$$

We will use the matrix product method to calculate these numbers, utilizing a path as shown on the right side of Figure 19. Although Theorem 4.3 was only stated for polygons, we can lift the triangulation to the universal cover to obtain a polygon with a zig-zag triangulation (in the default orientation), in which the appropriate odd elements are identified.

Since all λ -lengths are 1, let us abbreviate $E := E(1)$ and $A_\theta := A(1|\theta)$. The figure shows the example of z_4 . In general, the holonomy matrix product for z_n is

$$H_n = X^{n-2}E^{-1}, \quad \text{where} \quad X := E^{-1}A_\theta^{-1}\rho EA_\sigma\rho$$

Lemma 6.2. *The holonomy H_n , realizing the arc z_n , is given by*

$$\begin{aligned} H_n &= \left(\begin{array}{cc|c} -w_{n-1} & z_n & (z_n - 1)\sigma + w_{n-1}\theta \\ -z_{n-1} & w_{n-1} & (z_{n-1} - 1)\theta + w_{n-1}\sigma \\ \hline (z_{n-1} - 1)\sigma - w_{n-1}\theta & (z_n - 1)\theta - w_{n-1}\sigma & 1 - (\ell_{2n-4} - 2)\sigma\theta \end{array} \right) \\ &= \left(\begin{array}{cc|c} -(x_{2n-6} + y_{2n-6}\sigma\theta) & x_{2n-5} + y_{2n-5}\sigma\theta & (x_{2n-5} - 1)\sigma + x_{2n-6}\theta \\ -(x_{2n-7} + y_{2n-7}\sigma\theta) & x_{2n-6} + y_{2n-6}\sigma\theta & (x_{2n-7} - 1)\theta + x_{2n-6}\sigma \\ \hline (x_{2n-7} - 1)\sigma - x_{2n-6}\theta & (x_{2n-5} - 1)\theta - x_{2n-6}\sigma & 1 - (\ell_{2n-4} - 2)\sigma\theta \end{array} \right) \end{aligned}$$

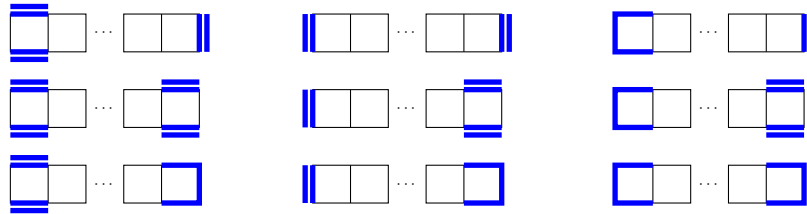
⁹The number y_k is really the weighted sum of all configurations which contain cycles, but those which have either more than one cycle or a cycle of even length have weight zero. This is because the same two odd variables appear repeatedly. See [MOZ22] for details.

Here ℓ_k denotes the k th Lucas number defined by $\ell_1 = 1$, $\ell_2 = 3$, and $\ell_k = \ell_{k-1} + \ell_{k-2}$ for $k \geq 3$.¹⁰

Proof. Consider the polygon in the universal cover of the cylinder surrounding the canonical path pictured in Figure 19. Note that this polygon, which has $2n - 2$ vertices, has a zig-zag triangulation with the default orientation. Furthermore, the holonomy has type 01 (in the sense of Definition 4.1). This ensures that the signs match those in Theorem 5.2.

Label the vertices $0, 1, \dots, 2n - 1$, as in Section 4.3 (note that since this picture is on the universal cover, $i = i + 2$). The snake graph G_T associated to this zig-zag triangulation is G_{2n-5} , a horizontal row of $2n - 5$ boxes. Therefore the snake graph $G_{\tilde{T}}$ described in Section 5 is G_{2n-3} . Since, as we mentioned above, this holonomy is of type 01, and since G_{2n-3} has an odd number of boxes, we will always have e_0 (resp. e_1) on the bottom (resp. left) side of the first tile, and e_N (resp. e_{N+1}) on the right (resp. top) of the last tile. Theorem 5.2 gives formulas for all nine entries of H_n in terms of subsets of double dimer covers of $G_{\tilde{T}} = G_{2n-3}$. Note that since we set all λ -lengths equal to 1, we can ignore the denominators in these expressions.

The following picture is the specialization of Figure 11 to the situation $\tilde{G} = G_{2n-3}$.



The $(1, 2)$ -entry (resp. the $(2, 1)$ -entry) has an obvious bijection with double dimer covers of G_{2n-5} (resp. G_{2n-7}), and hence by a result from [MOZ22] is equal to z_n (resp. z_{n-1}). Similarly, the $(1, 1)$ and $(2, 2)$ entries have obvious bijections with double dimer covers of G_{2n-6} , and so are equal to w_{n-1} .

The $(1, 3)$ -entry has a bijection with double dimer covers of G_{2n-4} containing a cycle which surrounds (at least) the first square. The first μ -invariant in \tilde{T} is θ , so cycles which surround an odd number of squares will end with a σ , and those surrounding an even number of squares will end with θ . According to Theorem 5.2, we additionally need to toggle the first θ , meaning the weights will contain only the μ -invariant at the *end* of the cycle. If the first cycle surrounds k tiles, the rest can be any double dimer configuration on the complement of the first $k + 1$ tiles (i.e. on G_{2n-5-k}). When k is odd, this is counted by $w_{n-\frac{k+1}{2}}$, and when n is even by $z_{n-\frac{k}{2}}$. Thus, we have that the $(1, 3)$ -entry is given by

$$(w_{n-1} + w_{n-2} + \dots + w_2)\sigma + (z_{n-1} + z_{n-2} + \dots + z_2)\theta.$$

Note that each w_i or z_i is of the form $x + y\sigma\theta$, so multiplying by either σ or θ annihilates the y -term, and so we may replace each z_i with x_{2i-5} and each w_i with x_{2i-4} , which are simply Fibonacci numbers. The following are well-known identities of Fibonacci numbers:

$$x_0 + x_2 + \dots + x_{2n-6} = x_{2n-5} - 1 \quad \text{and} \quad x_{-1} + x_1 + x_3 + \dots + x_{2n-7} = x_{2n-6}$$

¹⁰This quantity $\ell_{2n-4} - 2$ also equals $\kappa(W_{n-2})$, the number of spanning trees on the wheel graph with $(n-1)$ vertices (see [Mye71]).

The arguments for the $(2, 3)$, $(3, 1)$, and $(3, 2)$ -entries are similar. The signs in the bottom row come from Remark 4.9. In particular, this corresponds to a zig-zag triangulation where half of the odd variables are all set equal to σ and the other half all set equal to θ . Since we negate half of the odd variables in Remark 4.9, this means simply negating either σ or θ .

For the $(3,3)$ -entry, we use standard identities on Fibonacci and Lucas numbers: In particular, by Equation (4), we can express the $(3,3)$ -entry as $1 + \alpha\beta$, where α is the $(3,1)$ -entry and β is the $(3,2)$ -entry. We thus obtain

$$\begin{aligned} H_n(3,3) &= 1 + \left((x_{2n-7} - 1)\sigma - x_{2n-6}\theta \right) \left((x_{2n-5} - 1)\theta - x_{2n-6}\sigma \right) \\ &= 1 - \left(x_{2n-6}^2 - x_{2n-5}x_{2n-7} + x_{2n-5} + x_{2n-7} - 1 \right) \sigma\theta \end{aligned}$$

By Cassini's identity on Fibonacci numbers, we have the equality $x_{2n-5}x_{2n-7} - x_{2n-6}^2 = 1$ and another standard identity relating Fibonacci and Lucas numbers is $\ell_k = x_{k-3} + x_{k-1}$. Using this in the case of $k = 2n - 4$, we rewrite $H_n(3,3) = 1 + (\ell_{2n-4} - 2)\theta\sigma = 1 + (\kappa(W_{n-3}) - 2)\theta\sigma$ as desired. \square

Remark 6.3. In [MOZ22], we showed that z_n , defined as the generating function of double dimer covers of G_{2n-5} , is equal to the λ -length of certain arcs in an annulus, as described above. In the previous paper, we defined the w_n 's as double dimer generating functions for G_{2n-4} , and used them for algebraic calculations, but did not give a geometric interpretation. In Remark 11.17 and Conjecture 11.19 in [MOZ22], we suggested that the w_n 's should have a particular geometric meaning, which we are now able to verify. Comparing H_n from Lemma 6.2 with H_{ab} from Theorem 4.3, we see that the w_n 's can also be interpreted as certain λ -lengths. In particular, w_n is the λ -length of an arc which winds around the annulus $n - 2$ times, and has both endpoints on the same boundary component.

7. Geometric Interpretation

In this section, we will describe a more geometric interpretation of the results of this paper, in terms of the definitions of decorated super Teichmüller spaces given in [PZ19]. We take a viewpoint along the lines of [FG06] (section 11), which is slightly different than the viewpoint of [PZ19]. Some version of this viewpoint was also present in [Bou13], applied to super shear coordinates (rather than λ -lengths).

This alternative viewpoint is as follows. Let \mathcal{A} be the commutative super-algebra generated by λ -lengths and μ -invariants coming from some particular triangulation. The definitions of Penner and Zeitlin in [PZ19] are in terms of the Minkowski geometry of the free module $\mathcal{A}^{3|2}$, whereas our alternate viewpoint will be to instead view the elements of $\text{OSp}(1|2)$ acting on the free module $\mathcal{A}^{2|1}$ (by ordinary matrix-vector multiplication).

To connect the two viewpoints, we will give a map $s: \mathcal{A}^{2|1} \rightarrow \mathcal{A}^{3|2}$, which is equivariant with respect to the actions. This way, statements about the action may be stated in $\mathcal{A}^{2|1}$, where the action is simpler, and the statements will transfer over to $\mathcal{A}^{3|2}$.

In particular, our main goal in this section is to use this viewpoint to give geometric interpretations for the matrices $E(\lambda)$ and $A(h|\theta)$, and thus also the holonomy matrices $H_{a,b}$ of Definition 4.1 and Theorem 4.3.

The map $s: \mathcal{A}^{2|1} \rightarrow \mathcal{A}^{3|2}$, mentioned above, is given explicitly as follows:

$$s(x, y|\phi) := (y^2 - x^2, -2xy, y^2 + x^2 \mid -2y\phi, 2x\phi) \frac{1}{\sqrt{2}}.$$

Proposition 7.1. *The map $s: \mathcal{A}^{2|1} \rightarrow \mathcal{A}^{3|2}$ is equivariant with respect to the $\mathrm{OSp}(1|2)$ -actions.*

Proof. In [PZ19, section 1], each element $v \in \mathcal{A}^{3|2}$ was identified with a $2|1$ -by- $2|1$ matrix $Q(v)$, and the action of $\mathrm{OSp}(1|2)$ on $\mathcal{A}^{3|2}$ was defined by

$$g \cdot Q(v) = (g^{-1})^{\mathrm{st}} Q(v) g^{-1}.$$

Therefore one just needs to verify that

$$Q(s(g \cdot v)) = (g^{-1})^{\mathrm{st}} Q(s(v)) g^{-1}.$$

We omit this calculation, as it is straightforward. \square

Remark 7.2. Note that all entries of $s(x, y|\phi)$ are homogeneous quadratic expressions in x , y , and ϕ . It follows that $s(v) = s(-v)$ for all $v \in \mathcal{A}^{2|1}$. We may therefore think of the domain of the map s as the quotient $\mathcal{A}^{2|1} / \pm 1$, where vectors are identified with their negatives.

In [PZ19], the λ -lengths were defined in terms of a certain Minkowski inner product on $\mathcal{A}^{3|2}$. Specifically, they define $\lambda(a, b) := \sqrt{\langle a, b \rangle}$. Under this map s , the λ -lengths correspond to a certain bilinear form, which we now describe.

Definition 7.3. Define the map $\omega: \mathcal{A}^{2|1} \times \mathcal{A}^{2|1} \rightarrow \mathcal{A}$ as follows. If $v = (a, b|\phi)$ and $w = (x, y|\theta)$, then

$$\omega(v, w) := ay - bx + \phi\theta.$$

Remark 7.4. The map ω is the bilinear form defined by the matrix J (from Section 2), so by definition, $\mathrm{OSp}(1|2)$ is the group which preserves ω .

Proposition 7.5. *For any $v, w \in \mathcal{A}^{2|1}$, we have $\langle s(v), s(w) \rangle = \omega(v, w)^2$. In particular,*

$$\lambda(s(v), s(w)) = \sqrt{\omega(v, w)^2} = \pm \omega(v, w).$$

Lemma 7.6. *Let $v_1, v_2 \in \mathcal{A}^{2|1}$ with $\omega(v_1, v_2) = 1$. Then there is a unique matrix $g \in \mathrm{OSp}(1|2)$ whose first two columns are v_1 and v_2 .*

Proof. Let $v_1 = (a, b|\phi)$ and $v_2 = (x, y|\theta)$. We want to show there is some $v_3 = (\alpha, \beta, f)$ such that

$$\left(\begin{array}{cc|c} a & x & \alpha \\ b & y & \beta \\ \hline \phi & \theta & f \end{array} \right) \in \mathrm{OSp}(1|2).$$

If such a v_3 exists, it is unique by the relations defining $\mathrm{OSp}(1|2)$. In particular, equations (4), (8), and (9) say that α , β , and f are determined by v_1 and v_2 as follows:

$$f = 1 + \phi\theta, \quad \alpha = a\theta - x\phi, \quad \beta = b\theta - y\phi$$

However, the entries of the matrix must also satisfy equations (5), (6), and (7), so we must check that defining v_3 by the formulas above is consistent with these other three equations.

First is equation (5), which says that $ay - bx = 1 - \phi\theta$, or equivalently $ay - bx + \phi\theta = 1$, which is precisely our assumption that $\omega(v_1, v_2) = 1$. So we see this assumption is necessary in order to satisfy equation (5).

Next, equation (6) requires that $\phi = b\alpha - a\beta$. The right-hand side is

$$b\alpha - a\beta = b(a\theta - x\phi) - a(b\theta - y\phi) = (ay - bx)\phi.$$

But we already know from the discussion above that $ay - bx = 1 - \phi\theta$. Substituting this gives the desired result.

The calculation verifying equation (7), i.e. $\theta = y\alpha - x\beta$, is similar. \square

Definition 7.7. Let $\mathcal{A}_+^{2|1}$ be the set of vectors with non-zero bodies. That is

$$\mathcal{A}_+^{2|1} := \{(x, y|\phi) \in \mathcal{A}^{2|1} \mid x \neq 0 \text{ or } y \neq 0\}$$

Corollary 7.8. *The action of $\text{OSp}(1|2)$ on $\mathcal{A}_+^{2|1}$ is transitive.*

Proof. Let $v = (x, y|\phi) \in \mathcal{A}_+^{2|1}$. If there exists some w with $\omega(v, w) = 1$, then Lemma 7.6 tells us that there is some $g \in \text{OSp}(1|2)$ with $g \cdot e_1 = v$. If $x \neq 0$, we can choose $w = (0, x^{-1}|\phi)$, and if $y \neq 0$, we can choose $w = (-y^{-1}, 0|\phi)$. \square

Remark 7.9. The image of $\mathcal{A}_+^{2|1}$ under the map s was called the “special light cone” L_0^+ in [PZ19], and the decorated super Teichmüller space of a polygon is the configuration space of tuples of points in this set, modulo the diagonal action of $\text{OSp}(1|2)$. From the point of view described in this section, we instead consider configurations of points in $\mathcal{A}_+^{2|1}$, up to diagonal action of $\text{OSp}(1|2)$. Also, by Remark 7.2, we identify $v = -v$ in $\mathcal{A}_+^{2|1}$, since $s(v) = s(-v)$.

The following is a kind of standard form result (which can be seen in the argument used in the proof of Lemma 3.1 from [PZ19]). In order to state it, we first define the vectors $u := s(e_1)$ and $w = s(e_2)$ in $\mathcal{A}^{3|2}$.

Proposition 7.10. *Let $p, q \in L_0^+$ be two points in the special light cone with $\lambda = \lambda(p, q)$. There is some $g \in \text{OSp}(1|2)$ such that*

$$g \cdot p = u \cdot \lambda^2 \quad \text{and} \quad g \cdot q = w$$

Moreover, g is unique up to post-composition (i.e. left-multiplication) by ρ .

Proof. We will construct the inverse of the matrix g . Let $v_p, v_q \in \mathcal{A}^{2|1}$ be vectors such that $s(v_p) = p$ and $s(v_q) = q$. Then by Proposition 7.5, we know that $\omega(v_p, v_q) = \pm\lambda$. Since λ has positive body, it is invertible, and we may replace v_p with $v'_p = \pm v_p \cdot \frac{1}{\lambda}$, so that $\omega(v'_p, v_q) = 1$. Thus by Lemma 7.6, there is a matrix $g \in \text{OSp}(1|2)$ whose first two columns are v'_p and v_q . If e_1, e_2, ε are the standard basis vectors of $\mathcal{A}^{2|1}$, then this matrix acts by $g \cdot e_1 = v'_p$ and $g \cdot e_2 = v_q$. Proposition 7.1 says the map s is equivariant, so $g \cdot w = q$ and $g \cdot u = p \cdot \frac{1}{\lambda^2}$. Then clearly g^{-1} is the matrix described in the proposition.

Finally, we remark that the choices of v_p and v_q were not unique, since we may replace either (or both) by their negatives (Remark 7.2). If we replace $v_q \mapsto -v_q$, then when we re-scale v_p to get v'_p , it will also be negated. The overall effect is that the first two columns of g will be negated (but the third column will remain the same). This is the same as right-multiplication

by ρ . Since the matrix from the statement is g^{-1} , it will be unique up to left-multiplication by ρ . \square

Proposition 7.11. *Let $p, q \in L_0^+$ be in the standard form guaranteed by Proposition 7.10. That is, if $\lambda = \lambda(p, q)$, assume that $q = w$ and $p = u \cdot \lambda^2$. Then $E(\lambda)$ and $E(-\lambda) = E(\lambda)^{-1}$ are the only matrices $g \in \text{OSp}(1|2)$ such that $g \cdot p = q$ and $g \cdot q = p$.*

Proof. By Proposition 7.10, such a matrix is unique up to ρ . Note that $E(-\lambda) = \rho E(\lambda)$, so if we show that $E(\lambda)$ satisfies the conditions, then we are done.

If e_1, e_2, ε are the standard basis vectors of $\mathcal{A}^{2|1}$, then looking at the columns of $E(\lambda)$ shows that

$$E(\lambda) \cdot e_1 = e_2 \cdot \lambda^{-1} \quad \text{and} \quad E(\lambda) \cdot e_2 = -e_1 \cdot \lambda$$

Re-arranging the first equation gives $E(\lambda) \cdot (e_1 \cdot \lambda) = e_2$. Applying s to these equations, remembering that s is equivariant, and that $s(v \cdot \alpha) = s(v) \cdot \alpha^2$, we get

$$E(\lambda) \cdot (u \cdot \lambda^2) = w \quad \text{and} \quad E(\lambda) \cdot w = u \cdot \lambda^2 \quad \square$$

To prove the corresponding result about the $A(h|\theta)$ matrices, we will use the following lemma.

Lemma 7.12. *Let $p_1, p_2, p_3 \in L_0^+$, with $\lambda(p_i, p_j) = \lambda_{ij}$, and μ -invariant θ . Suppose the edge p_1, p_3 is in the standard form guaranteed by Proposition 7.10. That is, assume that $p_1 = u \cdot \lambda_{13}^2$ and $p_3 = w$. Then $p_2 = s(z)$, where*

- *If p_1, p_2, p_3 appear in clockwise order, then $z = \left(\lambda_{23}, \frac{\lambda_{12}}{\lambda_{13}} \mid \pm \nabla_{1,3}^2 \right)$.*
- *If p_1, p_2, p_3 appear in counter-clockwise order, then $z = \left(\lambda_{23}, -\frac{\lambda_{12}}{\lambda_{13}} \mid \pm \nabla_{1,3}^2 \right)$.*

In both cases, the sign of $\nabla_{1,3}^2$ cannot be determined from this information alone.

Proof. We will show the calculation for (a), and that of (b) is similar. Suppose that p_1, p_2, p_3 are in clockwise order. This means they are a “negative triple” (in the language of [PZ19]). Let $p_2 = s(z)$ for $z = (x, y|\alpha) \in \mathcal{A}^{2|1}$. Because this is a negative triple, the signs of x and y must be the same. By Proposition 7.5, we can deduce that

$$\lambda_{12} = \lambda(u \cdot \lambda_{13}^2, p_2) = \pm \omega(e_1 \cdot \lambda_{13}, z) = \pm y \cdot \lambda_{13}$$

$$\lambda_{23} = \lambda(p_2, w) = \pm \omega(z, e_2) = \pm x$$

Since $s(z) = s(-z)$, we may choose z so that $x = \lambda_{23}$ and $y = \frac{\lambda_{12}}{\lambda_{13}}$. In order to compare α with the μ -invariant θ , we need to put the triple p_1, p_2, p_3 into the standard form described in Lemma 3.3 and Lemma 3.5 of [PZ19]. This can be done with the following matrix:

$$g = \left(\begin{array}{cc|c} \sqrt{h_{12}^3} & 0 & 0 \\ 0 & \frac{1}{\sqrt{h_{12}^3}} & 0 \\ \hline 0 & 0 & 1 \end{array} \right)$$

The effect on z is then

$$g \cdot z = \left(1, 1 \mid \sqrt{h_{13}^2} \alpha \right) \cdot \frac{1}{\sqrt{h_{13}^2}}$$

By the definition of μ -invariant from [PZ19], we see that $\alpha = \frac{\pm\theta}{\sqrt{h_{13}^2}} = \pm\nabla_{1,3}^2$. By Corollary 3.4 in [PZ19], knowing the three points p_1, p_2, p_3 only determines θ up to sign.

The proof of (b) is the the same, except x and y have opposite signs, and there are some signs in the diagonal matrix g . \square

The following proposition is essentially a restatement of what is called the “*basic calculation*” in section 4 of [PZ19], but phrased in a way that highlights the significance of the A -matrices we defined in Section 3.

Proposition 7.13. *Let $p_i, p_\ell, p_k \in L_0^+$ in clockwise order, as in Figure 2, with λ -lengths a, b, e and μ -invariant θ , and suppose the edge p_i, p_k is in the standard form guaranteed by Proposition 7.10. That is, $p_i = u \cdot e^2$ and $p_k = w$. Then there is a unique point $p_j \in L_0^+$ such that*

- (a) *The triangle p_i, p_j, p_k has the λ -lengths and μ -invariant as in Figure 2.*
- (b) *The point p_j is defined by $A_{ij}^k \cdot p_j = u \cdot c^2$ (or $A_{ij}^k \rho \cdot p_j = u \cdot c^2$), depending on the orientation of the edge (i, k) . In other words, A_{ij}^k (or $A_{ij}^k \rho$) puts the edge (j, k) into standard position.*

Proof. Part (b) completely determines some point. We simply need to see that it satisfies the claim of part (a). Let us consider the case pictured in Figure 2, where the edge labeled “ e ” is directed $p_i \rightarrow p_k$. If $p_j = s(v)$, then v must be (up to sign) the first column of $\rho A_{ij}^k^{-1}$, multiplied by c , which gives

$$v = \left(-c, \frac{d}{e} \mid -\nabla_{i,k}^j \right)$$

Now, it is straightforward to check, using Proposition 7.5, that

$$\lambda_{ij} = \omega(v, e_1) \cdot e = d \quad \text{and} \quad \lambda_{jk} = \omega(v, e_2) = c,$$

and by the same calculation done in Lemma 7.12, we see that the μ -invariant \boxed{ijk} is σ . \square

We conclude with a discussion of how the holonomy matrices $H_{a,b}$ from Definition 4.1 and Theorem 4.3 can be interpreted in this geometric context. The main point is that we may represent a polygon as a configuration of points in $\mathcal{A}^{2|1}$ or $\mathcal{A}^{3|2}$, in such a way so that if the first edge (c_0, c_1) of the canonical path is in standard position, then the matrix H_{ab} is the transformation which puts the final edge (c_N, c_{N+1}) into standard position. Indeed, we can build this configuration of points inductively. Start by choosing three points for the first triangle using Proposition 7.10 and Lemma 7.12. Then Proposition 7.13 tells us how to choose the third point of the next triangle (which shares one side with the first one). Then we may use some product of E or A matrices to put the appropriate edge in standard position and continually use Proposition 7.13 to choose each subsequent point.

Acknowledgments

The authors would like to acknowledge the support of the NSF grants DMS-1745638 and DMS-1854162.

References

- [Bou13] Fabien Bouschbacher. *Shear coordinates on the super Teichmüller space*. PhD thesis, Université de Strasbourg, 2013.
- [FG06] Vladimir Fock and Alexander Goncharov. Moduli spaces of local systems and higher Teichmüller theory. *Publications Mathématiques de l’IHÉS*, 103:1–211, 2006.
- [FZ02] Sergey Fomin and Andrei Zelevinsky. Cluster algebras I: foundations. *Journal of the American Mathematical Society*, 15(2):497–529, 2002.
- [LMRS21] Li Li, James Mixco, B Ransingh, and Ashish K Srivastava. An introduction to supersymmetric cluster algebras. *The Electronic Journal of Combinatorics*, pages P1–30, 2021.
- [MOZ21] Gregg Musiker, Nicholas Ovenhouse, and Sylvester W. Zhang. An expansion formula for decorated super-Teichmüller spaces. *SIGMA. Symmetry, Integrability and Geometry: Methods and Applications*, 17:080, September 2021.
- [MOZ22] Gregg Musiker, Nicholas Ovenhouse, and Sylvester Zhang. Double dimer covers on snake graphs from super cluster expansions. *Journal of Algebra*, 2022.
- [MS10] Gregg Musiker and Ralf Schiffler. Cluster expansion formulas and perfect matchings. *Journal of Algebraic Combinatorics*, 32(2):187–209, 2010.
- [MW13] Gregg Musiker and Lauren Williams. Matrix formulae and skein relations for cluster algebras from surfaces. *International Mathematics Research Notices*, 2013(13):2891–2944, 2013.
- [Mye71] B Myers. Number of spanning trees in a wheel. *IEEE Transactions on Circuit Theory*, 18(2):280–282, 1971.
- [OS19] Valentin Ovsienko and Michael Shapiro. Cluster algebras with Grassmann variables. *Electron. Res. Announc. Math. Sci.*, 26:1–15, 2019.
- [Ovs15] Valentin Ovsienko. A step towards cluster superalgebras. *arXiv preprint arXiv:1503.01894*, 2015.
- [Ovs22] Valentin Ovsienko. Shadow sequences of integers: From fibonacci to markov and back. *The Mathematical Intelligencer*, pages 1–5, 2022.
- [Pen12] Robert C Penner. *Decorated Teichmüller theory*, volume 1. European Mathematical Society, 2012.
- [PZ19] RC Penner and Anton M Zeitlin. Decorated super-Teichmüller space. *Journal of Differential Geometry*, 111(3):527–566, 2019.
- [She22] Ekaterina Shemyakova. On super cluster algebras based on super Plücker and super ptolemy relations. *arXiv preprint arXiv:2206.12072*, 2022.
- [SV22] Ekaterina Shemyakova and Theodore Voronov. On super Plücker embedding and cluster algebras. *Selecta Mathematica*, 28(2):1–58, 2022.